

Magnetic Resonance and Computed Tomography Imaging of the Structural and Functional Changes of Pulmonary Arterial Hypertension

Mark L. Schiebler, MD,* Sanjeev Bhalla, MD,† James Runo, MD,‡ Nizar Jarjour, MD,§
Alejandro Roldan, PhD,¶ Naomi Chesler, PhD,|| and Christopher J. François, MD**

Abstract: The current Dana Point Classification system (2009) distinguishes elevation of pulmonary arterial pressure into pulmonary arterial hypertension (PAH) and pulmonary hypertension. Fortunately, PAH is not a common disease. However, with the aging of the First World's population, heart failure has become an important outcome of pulmonary hypertension, with up to 9% of the population involved. PAH is usually asymptomatic until late in the disease process. Although features that are indirectly related to PAH are found on noninvasive imaging studies, its diagnosis and management still require right heart catheterization. Imaging features of PAH include the following: (1) enlargement of the pulmonary trunk and main pulmonary arteries; (2) decreased pulmonary arterial compliance; (3) tapering of the peripheral pulmonary arteries; (4) enlargement of the inferior vena cava; and (5) increased mean transit time. The chronic requirement to generate high pulmonary arterial pressure measurably affects the right heart and main pulmonary artery. This change in physiology causes the following structural and functional alterations that have been shown to have prognostic significance: relative area change (RAC) of the pulmonary trunk, right ventricular stroke volume index, right ventricular stroke volume, right ventricular end-diastolic volume index, left ventricular end-diastolic volume index, and baseline right ventricular ejection fraction <35%. All of these variables can be quantified noninvasively and followed up longitudinally in each patient using magnetic resonance imaging to modify the treatment regimen. Untreated PAH frequently results in rapid clinical decline and death within 3 years of diagnosis. Unfortunately, even with treatment, fewer than half of these patients are alive at 4 years.

Key Words: hypertension, pulmonary, magnetic resonance angiography, multidetector computed tomography, thromboembolism, heart catheterization

(*J Thorac Imaging* 2013;28:178–195)

†Professor of Radiology, Mallinckrodt Institute of Radiology, Washington University, St. Louis, MO; *Associate Professor of Radiology, University of Wisconsin-Madison School of Medicine and Public Health; ‡Assistant Professor of Medicine, University of Wisconsin-Madison School of Medicine and Public Health; §Professor of Medicine, University of Wisconsin-Madison School of Medicine and Public Health; ¶Scientist, Department of Radiology, University of Wisconsin-Madison School of Medicine and Public Health; ||Professor of Biomedical Engineering, University of Wisconsin-Madison School of Medicine and Public Health; and **Associate Professor of Radiology, University of Wisconsin-Madison School of Medicine and Public Health, Madison, WI.

All authors and staff in a position to control the content of this CME activity and their spouses/life partners (if any) have disclosed that they have no financial relationships with, or financial interests in, any commercial organizations pertaining to this educational activity.

Reprints: Mark L. Schiebler, MD, Department of Radiology, University of Wisconsin-Madison School of Medicine and Public Health, 600 Highland Avenue, Madison, WI 53792-3252 (e-mail: mschiebleruwhealth.org).

CME Copyright © 2013 by Lippincott Williams & Wilkins

LEARNING OBJECTIVES

After completion of this activity, physicians should be better able to:

1. Identify the defining characteristics of pulmonary hypertension.
2. Identify those magnetic resonance imaging (MRI) techniques best suited for evaluation of patients with known or suspected pulmonary arterial hypertension.
3. Diagnose pulmonary hypertension using various imaging techniques.

INTRODUCTION

Pulmonary arterial hypertension (PAH) is a relatively rare phenomenon, with an estimated prevalence between 1/2000 and 1/50,000 adults.¹ It is rare for a radiologist to make the first diagnosis of this disease. One of the few times that a radiologist is expected to comment on the possibility of PAH, or other causes of pulmonary hypertension (PH), is when a routine chest radiograph is performed before ventilation/perfusion (V/Q) scanning for pulmonary embolism (PE) in patients with severe emphysema or chronic thromboembolic pulmonary hypertension (CTEPH). V/Q scanning is still viewed by many clinicians as the standard reference test for CTEPH. The purpose of the chest radiograph in this instance is to determine whether the dose of ^{99m}Tc-MAA should be reduced because of severe underlying lung disease.

Whereas physicians can screen for systemic arterial hypertension (high blood pressure) using a blood pressure cuff, there is no routine screening test for elevated pulmonary arterial pressure (PAP). Just as the renal arterioles show pruning and amputation of the capillary bed in long-standing systemic arterial hypertension resulting in renal failure, with chronic elevation of PAP the pulmonary arterioles must endure hypertension-induced smooth muscle hypertrophic narrowing, resulting in limitation of flow due to narrowing of these vessels and an increase in perfusion pressure. By the time of the first presentation of PAH, irreversible damage has often occurred to the vascular bed of the patient's lungs, resulting in dyspnea. Initiating medical treatment after symptoms have begun has only a modest role in forestalling death related to cor pulmonale.²

The terminology used for the many diseases responsible for causing elevated PAP is potentially confusing. The pathologic factors that cause an elevation in PAP are generally divided into precapillary and postcapillary. If the disorder is primarily of the precapillary pulmonary arteries, the classification of PAH is generally used; conversely, if the disorder is postcapillary the term PH is used. Although the

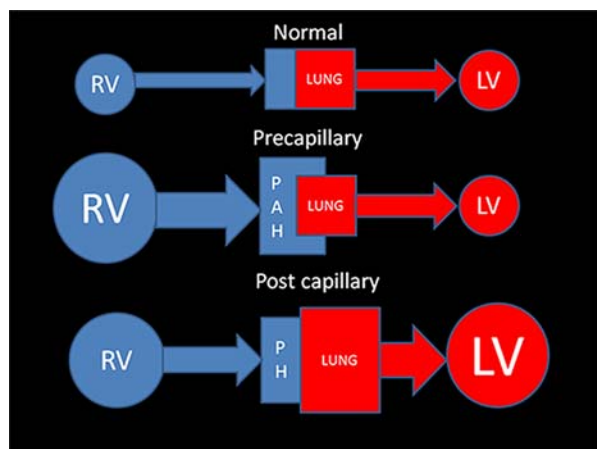


FIGURE 1. A simplified fluid mechanics model for understanding the differences between PAH and PH. Normal physiology: The Qp (pulmonary blood flow) matches the Qs (systemic blood flow); thus, the amount of blood entering the lungs is equal to the amount leaving the aorta. Precapillary: PAH: There is a problem in getting normal flow (or volume) to the last-order arteriole. PAH leads to back pressure, which reverberates retrograde into the RV. Curiously, PVOD (which is postcapillary) is categorized as a precapillary cause of PAH (Table 1, 1'). Post-capillary: PH: There is a limitation to the flow of oxygenated blood from the larger pulmonary veins all the way to the aortic valve that requires an increased capillary wedge pressure. This is typically associated with left heart dysfunction and enlargement. There is secondary enlargement of the right heart and pulmonary arteries that occurs late in this form of PH. LV indicates left heart including the atrium and ventricle; RV, right heart including the ventricle, atrium, and systemic veins.

fluid mechanics diagram shown in Figure 1 is an oversimplification, it can act as a heuristic device to group these 2 major causes of elevated PAP into precapillary and postcapillary causes. The Dana Point Classification (2009) (Table 1) is the most recent clinical system for the categorization of this disorder.³ The aim of this new classification system is to shift from a strictly causative one based on pathophysiology to a treatment-based scheme that sorts the many diseases that cause an elevated PAP on the basis of treatment.

By definition, PAH, and other types of PH, is a diagnosis that is invasively established after right heart catheterization (RHC). The three current invasive criteria by which this diagnosis can be made are: (a) mean PAP (mPAP) > 25 mm Hg at rest; (b) pulmonary capillary wedge pressure < 15 mm Hg; or (c) pulmonary vascular resistance (PVR) > 3 Wood units (300 dyn·s/cm⁵).⁴ Acutely, the right heart cannot generate systolic PAP > 40 mm Hg.⁵ Therefore, any systolic PAP > 40 mm Hg implies chronic PAH. The severity level of PAH is categorized by the invasive measurement of mPAP at rest in the supine position during RHC: severe PAH, > 50 mm Hg; moderate PAH, 30 to 50 mm Hg; and mild PAH, > 25 and < 30 mm Hg.

The number of newly diagnosed causes of PAH pales in comparison with the frequency of the many conditions that cause PH: ischemic cardiomyopathy with left-sided heart failure, chronic obstructive pulmonary disease, asthma, pneumonia, lung cancer, PE, and living at very high altitudes (Table 1). The prevalence (proportion of the population with PAH) of this disease is probably

TABLE 1. Updated Clinical Classification of PAH and Other Causes of PH (Dana Point 2009)³

1. PAH	
1.1 Idiopathic	1.2.1 BMPR2
1.2 Heritable	1.2.2 ALK1, endoglin
	1.2.3 Unknown
1.3 Drug and toxin induced	
1.4 Associated with	1.4.1 Connective tissue diseases
	1.4.2 HIV infection
	1.4.3 Portopulmonary hypertension
	1.4.4 Congenital heart disease (shunts)
	1.4.5 Schistosomiasis
	1.4.6 Chronic hemolytic anemia
1.5 Persistent PH in the newborn	
1.' Pulmonary veno-occlusive disease (PVOD) and/or pulmonary capillary hemangiomatosis (PCH)	
2. PH from left-sided heart disease	
2.1 Systolic dysfunction	
2.2 Diastolic dysfunction	
2.3 Valvular disease	
3. PH from lung disease and/or hypoxia	
3.1 Chronic obstructive pulmonary disease	
3.2 Idiopathic pulmonary fibrosis	
3.3 Other pulmonary disease with mixed restrictive and obstructive pattern	
3.4 Sleep-disordered breathing	
3.5 Alveolar hypoventilation disorder	
3.6 Chronic exposure to high altitude	
3.7 Developmental anomalies	
4. Chronic thromboembolic pulmonary hypertension (CTEPH)	
5. PH unclear cause	
5.1 Hematologic	Splenectomy, Myeloproliferative disorders
5.2 Systemic disease	Sarcoidosis, Pulmonary Langerhans cell Histiocytosis, Lymphangiomatosis, Neurofibromatosis, Vasculitis
5.3 Metabolic disorders	Glycogen storage disease, Gaucher disease, Thyroid disorders
5.4 Others	Tumoral obstruction, Fibrosing mediastinitis, Chronic renal failure on dialysis

underestimated in both developed and developing countries, as the definitive diagnosis is usually made late in the disease course when patients already have severe dyspnea.^{1,6} PAH is one of the few vascular diseases that occurs more commonly in women (1.7:1).⁷ The REVEAL study of PAH found that, in the United States, women were affected 80% of the time.⁸ This disorder can be inherited and has been linked to genetic mutations. Although an estimate of the prevalence of this disease is difficult to make, it has been reported that there are > 100,000 individuals in the United States with PAH; one study has reported the figure to be as high as 1:2000 individuals.⁹ Other countries have similar estimates of PAH prevalence: 2.6 cases/100,000 individuals in the Scottish Isles and 1.5 cases/100,000 individuals in France.¹⁰ In the French registry, the relative frequency of diseases causing PAH was

TABLE 2. Comparative Analysis of Diagnostic Imaging Tests for the Evaluation of Common Imaging Findings Associated With Early Cor Pulmonale Using a Nominal Scale for Efficacy

Structure	Finding	NCCT	CTA*	MRI
Subcutaneous fat	Morbid obesity	1	1	2
SVC	Enlarged	4	4	4
Azygous vein	Reflux of contrast	0	4	4
	Large	1	1	1
IVC	Large	1	2	3
	Contrast reflux	0	4	3
RA	Large	2	2	4
RA pressure	>4 mm Hg	1	1	2
Interatrial septum	Bowing from right to left	1	2	4
	Open PFO	0	1	2
	ASD	1	1	3
TV	TR jet velocity	0	0	4
	TR volume	0	0	4
	TAPSE	0	0	3
	e to a ratio	0	0	3
RV	RVH	2	2	4
	Enlarged RV	2	2	4
	Abnl RV motion	0	1	4
	Mass in grams	0	0	4
	Abnl RV minor axis	2	3	4
	RVEDV _{index}	0	0	4
	RVEF	0	0	4
	RVSV _{index}	0	0	4
	McConnell sign	0	0	3
IVS	"D" shape	1	1	4
	DCE	0	1	4
	VSD	1	1	4
	Eisenmenger syndrome	2	2	4
PV	PR (+/-)	0	0	4
	PR volume	0	0	4
PA	Enlarged PT	4	4	4
	PAP > 25 mm Hg at rest	0	0	2
	Acute embolism	1	4	3
	Chronic embolism	1	4	2
	Compliance	0	0	3
	Pulmonary flow (Qp)	1	1	4
	Oxygen saturation	0	0	0
	Right to left shunt fraction	0	0	4
PA branches	Enlarged interlobar arteries	4	4	4
	Pruning of PAs	3	3	3
	MTT	0	1	3
	Pulmonary perfusion	0	1	3
	PDA	1	3	4
Capillary obstruction	Microvasculature emboli (CTEPH)	1	1	1
	PCH	4	4	0
Microvasculature capillary shunts	Hepatopulmonary syndrome	0	0	0
Pulmonary veins	PVOD	4	4	0
	Wedge pressure	0	0	0
	Oxygen partial pressure	0	0	0
	PAPVR	2	3	4
Left heart	Left atrial fibrillation	0	0	1
	Large	2	2	4
	Mitral valve disease	2	2	4
	LV failure	2	2	4
	LVEDV _{index}	0	0	4
	LVESV _{index}	0	0	4
	LVSV	0	0	4

TABLE 2. (continued)

Structure	Finding	NCCT	CTA*	MRI
Aorta	AV stenosis	2	2	4
	Aortic flow (Qs)	0	0	4
	Shunt fraction (Qp/Qs)	0	0	4
Lung parenchyma	Ventilation	1	1	4
	Air trapping	4†	2	4‡
	Mosaic pattern	4	3	0
	Fibrosis	4	4	1

0 indicates not useful; 1, occasionally useful; 2, minimally useful; 3, moderately useful; and 4, very useful.

*CTA not cardiac gated.

†Xenon CT ventilation (morbid obesity may be associated with metabolic syndrome, diabetic cardiomyopathy, and sleep-disordered breathing).

‡MRI ventilation using hyperpolarized gas.

Abnl indicates abnormal; ASD, atrial septal defect; DCE, delayed contrast enhancement; e to a ratio, atrial filling pattern on RHC pressure volume loop; IVC, inferior vena cava; IVS, interventricular septum; LVESV_{index}, LV systolic volume index; LVSV, LV stroke volume; PA, pulmonary artery; PAPVR, partial anomalous pulmonary venous return; PDA, patent ductus arteriosus; PFO, patent foramen ovale; PR, pulmonary valve regurgitation; PT, pulmonary trunk; PV, pulmonary valve; RA, right atrium; RVEDV, RV end-diastolic index; TAPSE, tricuspid valve annular plane excursion; TV, tricuspid valve; VSD, ventricular septal defect.

shown to be as follows: 39.2%, idiopathic (Dana Point 1.1); 15.3%, connective tissue diseases (Dana Point 1.4.1); 11.3%, congenital heart disease (Dana Point 1.4.4); 10.4%, portopulmonary hypertension (Dana Point 1.4.3); 9.5%, anorexigen (Dana Point 1.3); and 6.2%, human immunodeficiency virus associated (Dana Point 1.4.2).^{1,6}

INITIAL CLINICAL PRESENTATION

PAH is an insidious disease that relentlessly diminishes the patient's cardiopulmonary reserve at an occult rate. The progression of disease remains below the threshold of visualization of symptoms for many years. The clinical presentation is variable, with the following findings found in decreasing order of frequency: dyspnea, positive antinuclear antibody, syncope, fatigue, and Raynaud's syndrome. Individuals present about 2 years after the onset of symptoms, with a mean age at onset of 36 years (± 15 y). In the United States, recent data show that the average age at diagnosis is now much older at 50.1 years.⁸ The mean treated survival time from PAH is now estimated to be 3.6 years.⁷

The incidence of other diseases that cause PH is much higher than the incidence of those that cause PAH. This is because diseases that affect the left side of the heart are included as causes of PH. When transthoracic echocardiography (TTE) is performed at the time of the initial diagnostic workup, it typically shows advanced disease as evidenced by the following echocardiographic findings: (1) right ventricular hypertrophy (RVH); (2) tricuspid regurgitation (TR); and (3) elevated right atrial pressure. In an echocardiographic study of PH performed in Australia by Strange and colleagues in a cohort of 10,314 patients using the jet of TR to estimate pulmonary arterial systolic pressure (ePASP) >40 mm Hg, the combined incidence of elevated PAP was found to be 9.1% [95% confidence interval (CI), 8.6%-9.7%] of their study population. Thus, this is really not such a rare disease after all. They found the overall "indicative" prevalence for all forms of elevated PAP (as measured by ePASP) to be 326/100,000 inhabitants, with left-sided heart disease-associated

PH being the most common form, with an “indicative” prevalence of 250 cases/100,000.² In their series, there were 15 cases of PAH/100,000 inhabitants.² This echocardiographic determination of PAP by ePASP yields 10 times the frequency of the French registry numbers (1.5/100,000), which were established by RHC.^{1,6} Fifteen percent of the cases of PH identified using ePASP by Strange et al² in Australia (144 individuals) had no identifiable cause for their PH. Thus, if we use only the RHC data for the determination of PAH, the incidence is around 15 cases/million. In contrast, if the definition for the determination of elevated PAP is broadened to include ePASP by echocardiography, the incidence of all causes of elevated PAP (both PAH + PH) increases to a minimum of 3260/million.²

In the United States, the number of deaths and hospitalizations attributable to PAH has increased.¹¹ Although there are some causes of elevated PAP that are amenable to surgical therapy (CTEPH and left to right shunts-PH), chronically elevated PAP frequently leads to early death, irrespective of the cause. Strange et al² found a mean time to death of 4.1 years (95% CI, 3.9-4.3 y) in a nonselected cohort of patients with ePASP > 40 mm Hg followed up in Australia. The death rate from PAH was found to be proportional to the severity of the disease as estimated from the ePASP, with severe PAH shortening the lifespan by an average of 1.1 years as compared with mild PAH.² In their patients, PAH increased all-cause mortality, but patients with PH secondary to left-sided heart disease had the worst prognosis.² Curiously, those patients with idiopathic PAH and receiving disease-specific treatment had a slightly better prognosis compared with patients with postcapillary disease.²

Currently, there are 3 clinically derived variables associated with survival in PAH: (1) the 6-minute walk test; (2) the New York Heart Association class; and (3) the mixed venous oxygen saturation level. Without treatment, the mean duration of survival after diagnosis of PAH is a very short 2.8 years.¹² The biomarkers that have been found to have prognostic value in patients with PAH include: brain natriuretic peptide, N-terminal probrain natriuretic peptide, cardiac troponin T, serum creatinine, uric acid, and the diffusing capacity of carbon monoxide. The hemodynamic features known to have prognostic importance for PAH survival include: mPAP, right atrial pressure, cardiac index, PVR, pulmonary arterial capacitance, mixed venous oxygen saturation level, systolic blood pressure, and heart rate.

ACUTE PH

The most common cause of acute PH is related to pulmonary embolism (PE).¹³ If the patient's cardiopulmonary reserve has been sufficiently compromised, these events can prove to be fatal, particularly if there is associated systemic hypotension (Qs) caused by massive pulmonary artery obstruction from PE resulting in a lack of life-sustaining pulmonary perfusion (Qp). This disorder has a very high mortality rate (18%) for hospital inpatients.¹⁴ The findings of acute PH related to PE are similar for both magnetic resonance angiography (MRA) and computed tomography angiography (CTA). These changes in the cardiopulmonary physiology and their associated imaging correlates as demonstrated on noncontrast computed tomography (NCCT), CTA, and MRI are fully detailed in Table 2.

The use of CTA has revolutionized the noninvasive diagnosis of PE and is now the gold standard test by which all others are judged.^{15,16} There are many cases of acute PH

caused by massive amounts of embolic clot that may show the following findings: interventricular septal (IVS) bowing; increased pulmonary artery diameter/aorta diameter ratio (PAD/AoD); increased superior vena cava (SVC) diameter; enlargement of the pulmonary trunk; enlargement of the right and left pulmonary arteries; pulmonary infarction; pleural effusion; enlargement of the right ventricle (RV); increased short axis of the RV [larger than the short axis of the left ventricle (LV)]; RV/LV ratio; pulmonary obstruction index¹⁶; enlargement of the right atrium; and venous contrast reflux into the hepatic venous system or azygous vein (Table 3). In a recent retrospective multivariate regression analysis of 152 patients with acute PE, Heyer et al²⁷ showed that, of the many variables assessed on CTA examinations in patients with acute PE, the most significant for determining whether the patient would require mechanical ventilation was hepatic venous reflux into the inferior vena cava ($P < 0.008$) (Table 4). In that series, using a univariate linear regression model, mortality was determined to be significantly associated with the pulmonary obstruction index (POI), short-axis RV/LV ratio, diameter of the SVC, venous contrast reflux into the azygous vein, and venous contrast reflux into the IVC (respective P values: < 0.001 , < 0.001 , < 0.015 , < 0.03 , and < 0.015) (Table 4).²⁷⁻²⁹ Enlargement of the right side of the heart in its major and minor axes without associated hypertrophy can be an important discriminator for distinguishing acutely elevated PAP from more chronic causes. In chronic PH, there is typically an enlarged RV demonstrating hypertrophy (until the RV fails) with associated enlargement of the main pulmonary artery such that its diameter is greater than that of the aorta at the same level.³²

The use of MRA as a solitary imaging method in the setting of acute PE has been thoroughly investigated, and it has been found to have lower efficacy for the diagnosis of PE compared with CTA (Fig. 2).^{33,34} The PIOPED III investigators found a sensitivity of 78% (95% CI, 67-86) with a specificity of 99% (95% CI, 96-100) for MRA in the diagnosis of PE (when compared with a contemporaneous CTA). The PIOPED III investigators concluded that MRA for the primary diagnosis of PE should be reserved for those centers with significant technical experience in this modality and that MRA can be considered an alternative test for PE in those patients with anaphylactic reactions to iodinated contrast material.³³ The IRM-EP study also showed modest efficacy for the diagnosis of acute PE using MRI, mirroring the results of the PIOPED III study.^{33,34}

The clinical adoption of MRA for the primary diagnosis of PE has been hampered by its inability to detect subsegmental PE. This is because the lack of signal intensity in the normal lung provides little to no background signal intensity by which to observe these occluded small vessels. The final result is a low signal intensity–occluded vessel that is indistinguishable from the surrounding low–signal intensity lung.³⁴ This problem is somewhat mitigated when perfusion imaging is used. Routine dextro-phase MRA acquisitions can show dorsal perfusion defects associated with a PE (Fig. 2). Kalb et al³⁵ have recently reported their experience using a combined approach with MRI, MRA, and perfusion MRA for the diagnosis of PE. In their series of 22 patients using a triad of MR imaging sequences [3-dimensional (3D) gradient recalled echo, MRA, and true fast imaging with steady-state precession], all read in combination with one another, the overall

TABLE 3. Efficacy of Pulmonary Artery Measurements From NCCT Scans for Predicting the Presence of PAH

References	PAH Cases	Normal Controls	PT Size (mm):		P	Sensitivity	Specificity	MPA _{index} :		P
			Abnl	Cutoff Normal				Abnl	Normal	
Kuriyama et al ¹⁷	32	26	—	—	—	—	—	—	—	0.001
			28.6	—						
Frank et al ¹⁸	23	8	—	—	0.02	—	—	18 ± 3	12 ± 1	< 0.008
Murray et al ¹⁹	12	8	36 ± 8	—	0.02	—	—	28 ± 7 mm	—	< 0.0001
			29 ± 3	—				17 ± 2 mm	—	
Edwards et al ²⁰	12	100	35 ± 3	—	< 0.01	0.58	0.95	—	—	—
			33	—						
			27 ± 3	—						
Sanal et al ²¹	51 (Echo)	139	—	—	—	0.75	0.75	—	—	—
			28.6	—						
Beiderlinden et al ²²	95 acute PH	8	—	—	< 0.001	0.54	0.63	—	—	—
			29 ± 4	—						
Zisman et al ²³	65 PAH	257	33 ± 3.7	—	0.19	—	—	18 ± 3 mm	—	< 0.29
			31 ± 3.7	—				17 ± 3 mm	—	
Ghanem et al ²⁴	19 PAH	18	27 ± 9	—	0.39	—	—	—	—	—
			25 ± 8	—						
Lingurarur et al ²⁵	20 (SCD)	20	34 ± 7	—	< 0.001	—	—	—	—	—
			27 ± 3	—						
Tan et al ²⁶	36	9	35 ± 6	—	—	0.87	0.89	—	—	—
			29	—						
			27 ± 2	—						

Abnl indicates abnormal; MPA_{index}, main pulmonary artery index; Echo, echocardiography; SCD, sickle cell disease.

sensitivity and specificity for the diagnosis of individual pulmonary emboli were 84% and 100%, respectively.³⁵

Our group has been performing MRA for the primary diagnosis of PE since September 2007 (Fig. 2). To date, we have successfully performed over 500 MRA examinations in dyspneic patients, and it is part of the clinical imaging paradigm for this disorder at our institution. We use this test

primarily in young women, children, and patients with contrast allergies. Recently, we completed a retrospective review of our outcomes data. Using electronic medical records pertaining to 3 months' follow-up in 167 patients, we found the following respective test effectiveness values (95% CI) for accuracy, sensitivity, specificity, positive predictive value, and negative predictive value (NPV): 97% (92-99), 82% (64-97),

TABLE 4. Imaging Biomarkers Predictive of Mortality Using a Univariate Analysis in Patients With Elevated PAP

References	Clinical Population	Imaging Method	Image-based Biomarker	P
Heyer et al ²⁷	Acute PH PE	CTA	POI RV/LV ratio	<0.001
			SVC diameter	0.015
			Azygous vein contrast reflux	0.03
			IVC contrast reflux	0.015
Van de Veerdonk et al ²⁸	PAH	MRI	RVSF < 35% at baseline	0.001
			ΔRVEF	0.014
			RVEDV ≥ 84 mL/m ²	0.011
			RVSF _{index}	0.006
Van Wolferen et al ²⁹	PAH	MRI	RVEF	0.015
			RVEDV _{index}	0.037
			LVEDV _{index}	0.019
			TAPSE	<0.01
Mathai et al ³⁰	PAH scleroderma	TTE		<0.01
Gan et al ³¹	PAH	MRI	RAC	<0.001

RV/LV ratio indicates short axis of RV in mm/short axis of LV in mm measured at the largest portion of the RV on axial imaging (not an angled 4-chamber view); POI, pulmonary obstruction index; TAPSE, tricuspid annular plane excursion.

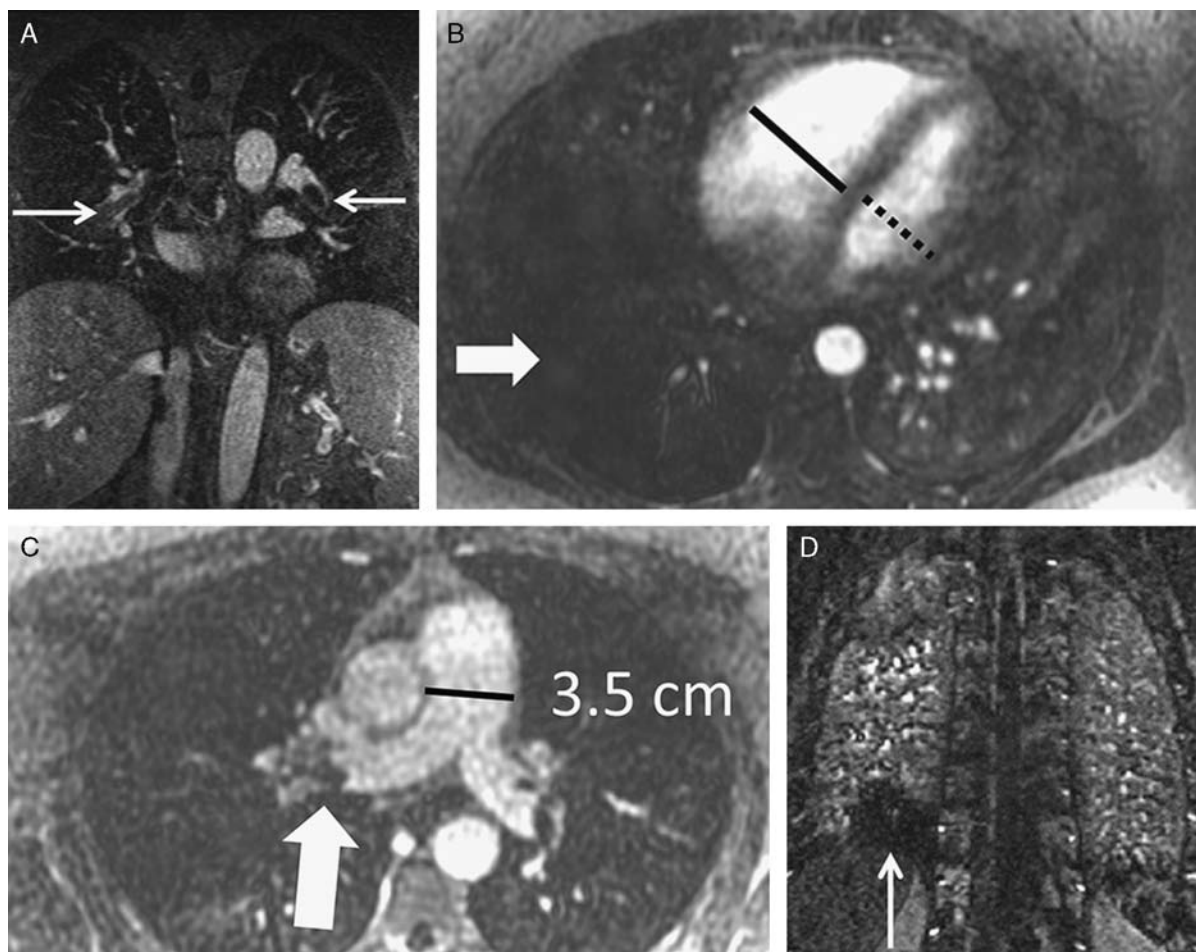


FIGURE 2. PE as a cause of acute PAH. A, Coronal MRA showing bilateral pulmonary emboli (white arrows). B, Right heart strain as seen on nongated single 17-second breath-hold MRA with an increase in the short axis of the RV (solid line) as compared with the LV (dotted line) and decreased perfusion of the right lower lobe (RLL). C, Increased size of the pulmonary trunk (black measurement caliper - 3.5 cm) in acute PH caused by PE (thick white arrow). PAD measurements of >3.0 cm have some utility in suggesting the possible presence of elevated PAP; however, not all enlarged pulmonary arteries are associated with increased PAP. The PAD indexed to body surface area has better sensitivity and specificity for the presence of abnormal PAP. D, Another patient with a small RLL perfusion defect from a subsegmental PE (white arrow).

100% (96-100), 100% (83-100), and 97% (92-99).³⁶ These effectiveness data are very similar to the efficacy data found by PIOPED III.³³ The key number from this MRA effectiveness study is an NPV of 97%, which is close to the 99% NPV value found for CTA.¹⁵

The reader should ask a critical question at this juncture: is finding subsegmental PE clinically significant? Recent data from Carrier et al³⁷ show that the death rate from PE has not decreased with the use of CTA-PE, and as such they have concluded that “the diagnosis of subsegmental PE may not be clinically significant.” Stated in another way, for those individuals without procoagulant conditions, the body is able to safely thrombolize subsegmental PEs without intervention. Therefore, as corroborated by our initial outcome data, even though MRA-PE is less sensitive for the detection of subsegmental PE, it is still an acceptable alternative test to CTA-PE, as this small amount of clot has heretofore not been shown to be clinically significant for patient survival.³⁶ There are, however, many clinicians who will actively anticoagulate patients with a single subsegmental PE. The risks and benefits of anticoagulation for PE needs to be carefully

considered, particularly for older individuals, as anti-coagulation therapy can be associated with significant morbidity and even death.

The lack of diagnostic medical radiation to the chest is one of the key advantages of pulmonary MRA. In younger individuals, there is a higher degree of radiation sensitivity. It would be beneficial to have a nonionizing alternative to CTA and nuclear medicine V/Q scanning for younger patients and female patients, for whom the possible diagnosis of PE needs to be evaluated. Pijpe et al³⁸ have recently shown that even a mammogram in those patients with BRCA1/2 mutations has a measurable effect on induction of breast malignancy. They have found the hazard ratio to be 1.63 in this group after only 0.002 Gy of diagnostic medical radiation. They have also demonstrated a dose-response relationship between the induction of malignancy and the amount of diagnostic medical radiation used. This indicates that, for this distinct population of at-risk patients (BRCA1/2), there is no linear dose threshold for the induction of malignancy using diagnostic medical radiation. In addition, these authors have found some preliminary evidence that exposure to CT before the age of 30, in this

at risk group, could be associated with an increased risk for breast cancer [hazard ratio 2.36 (95% CI, 0.71-7.88)].³⁸ In an emergency situation, the status of a particular patient's BRCA1/2 genotype is frequently unknown. From the perspective of medical radiation safety, one can certainly make the argument that at those centers with sufficient technical expertise, MRA-PE examinations should at least be offered as an alternative to CTA for young women and children with a positive D-dimer and clinical risk factors for PE (eg, Factor V Leiden deficiency, oral contraceptive use).

CHRONIC PAH LEADS TO DEATH FROM COR PULMONALE

There is a common fatal pathway for all patients with chronic PAH: cor pulmonale (Fig. 3).³⁹ Over time, this

elevated pulmonary arterial afterload induces RVH. In the short term, the RV is able to compensate for the demands of increased PAP. However, ultimately, failure occurs when the RV is no longer able to keep up with the insatiable need for more PAP as the PVR continues to worsen. The downward death spiral continues unabated as PAH progresses due to less blood returning from the lungs to the left side of the heart, resulting in a critical loss of cardiac output and coronary perfusion. A second major problem develops from the back pressure due to worsening central venous hypertension. As major organs fill up with interstitial fluid, tissue perfusion suffers and there is an increased demand for even higher systemic pressure of oxygenated blood. This in turn activates the adrenal axis of renin and angiotensin to raise the systemic systolic blood pressure—the last thing an LV needs is more demand to generate pressure in the face of diminishing

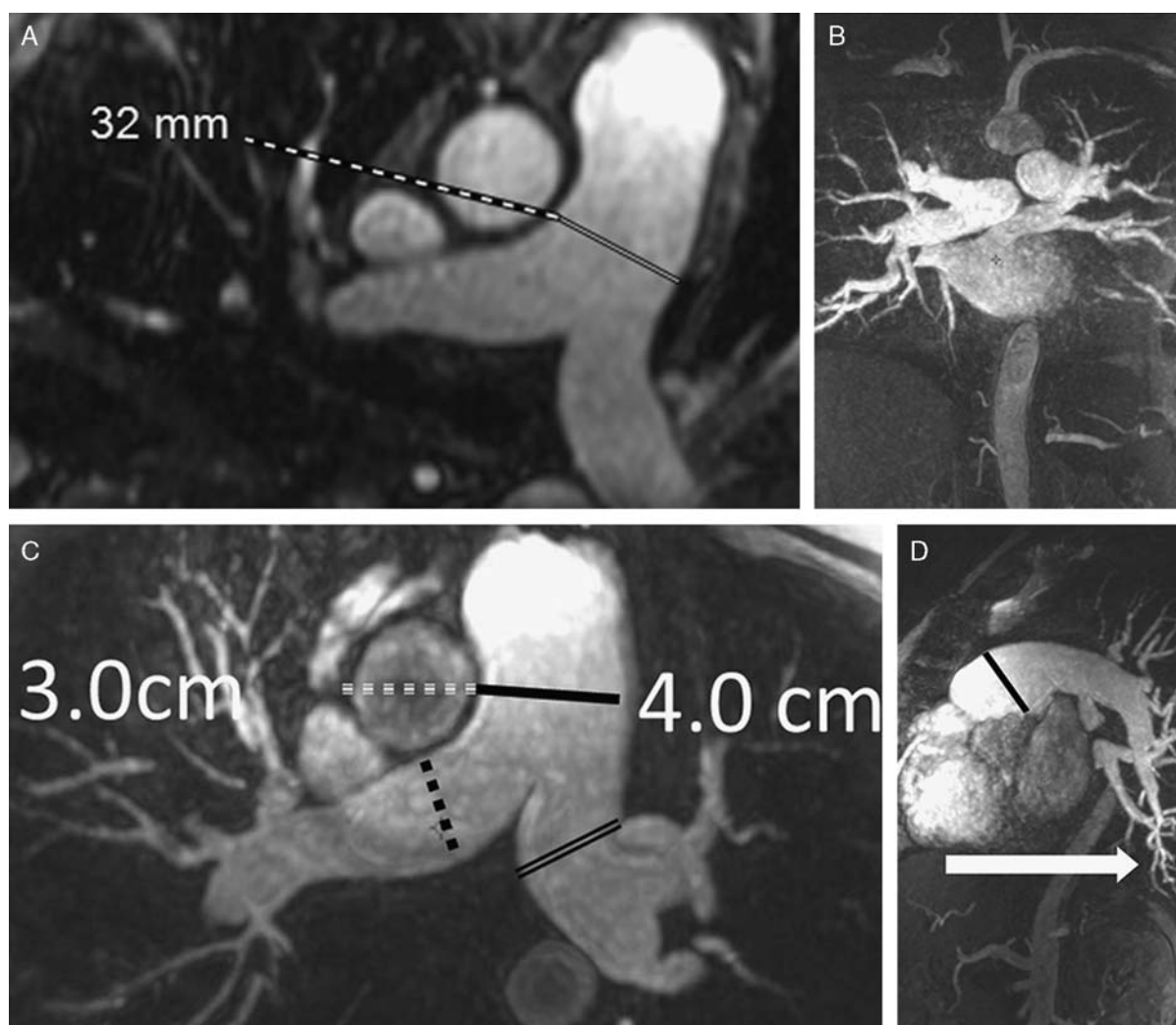


FIGURE 3. MRA of chronic PAH from systemic sclerosis. A, A single 1.2-mm-thick axial 3D MRA slice of a slightly enlarged pulmonary trunk in the setting of mild chronic PAH from scleroderma. Measurement of Pulmonary trunk (white solid line) is denoted by the dashed white and black line connecting to the workstation measurement of 32 mm. B, A coronal thick slab MRA MIP of advanced PAH from systemic sclerosis. C, A thick slab MIP axial MRA of advanced PAH from systemic sclerosis showing an enlarged pulmonary trunk (thick black line) at 4 cm and a normal-sized ascending aorta (dashed white line) with enlargement of both the right (dashed black line) and left main pulmonary arteries (double thin black lines). D, A sagittal thick slab double-oblique thick slab MIP angled to the left lower lobe pulmonary artery (black line) of advanced PAH from systemic sclerosis showing vessel amputation and a corkscrew path (arrow) to the lung periphery.

cardiopulmonary reserve and less coronary artery flow. For a while, the RV and LV are able to adapt to the demands of these new pressure volume loops. However, the good news is short lived in the setting of progressive PAH because the RV is not able to keep up with the ratcheting up of demands for increased pressure (increasing load) from worsening of the mPAP. Thus, the condition of the patient starts to deteriorate, as the patient's body is no longer able to sustain the basic needs of tissue oxygenation and waste (nitrogen and CO₂) disposal. This is the reason that death occurs so rapidly in these patients.

RV CHANGES INDUCED BY CHRONICALLY ELEVATED PAP

There is an essential commonality in all of the imaging findings of the RV in the setting of elevated PAP that simply reflects the underlying biomechanics of this "piggy back" ventricle straining to generate higher than normal pressure. Specifically, the three *primary* findings indicative of right-sided heart strain are: (1) dyskinesia of the RV free wall next to the atrioventricular groove seen at echocardiography or standard steady-state free-precession (SSFP) cardiac-gated MRI (McConnell's Sign - seen at echocardiography)⁴⁰; (2) straightening of the IVS indicating higher RV pressure than LV pressure at that point in the cardiac cycle (CTA, MRA); and/or (3) bowing of the IVS from the RV to the LV at systole indicating that RV pressure (or volume) is higher than LV pressure (or volume) at that point in the cardiac cycle. This IVS bowing can also be seen in diseases that do not have increased PAP, such as with constrictive pericarditis during inspiration, wherein the diastolic inflow volume of the RV exceeds the diastolic inflow volume of the LV, resulting in bowing of the septum toward the LV during diastolic filling. There are also *secondary* signs of RV strain: (A) velocity of the TR jet increases proportionally with the severity of PAP elevation⁴¹; (B) progressive RVH; (C) increasing RV dilation (larger minor and major axes); (D) increase in RV end-diastolic volume index (RVEDV_{index}); and occasionally (E) pericardial effusion.⁴² The amount of RVH (millimeters of wall thickening) is dependent on the chronicity of the elevated PAP and how much excess volume is present at end diastole. An RV free wall thickness of > 5mm is considered to be hypertrophic. Just as in the case of LV failure associated with diseases causing severe afterload, as the RV begins to fail from the increased afterload of chronically elevated mPAP, the RVH gives way to dilation with an overall increase in the RVEDV_{index} (Tables 2–4).

NCCT FINDINGS OF ELEVATED PAP

Standard NCCT without cardiac gating of the chest reveals a wealth of information about the cardiopulmonary system (Tables 2, 3).^{17–26} Over the last 20 years, 2 areas in the mediastinum have garnered a great deal of attention in those patients suspected of having PAH: the pulmonary trunk and the right and left main pulmonary arteries.²⁰ These have been measured under many conditions and have been found to be larger in PAH (Tables 2–3).^{17–26} Devaraj et al⁴³ have recently shown that the right and left PADs exceeding 1.8 cm are the best predictors of mortality in patients with bronchiectasis, as these CT findings are considered to be a biomarker for elevated PAP. Some authors have recently proposed using the PAD/AoD ratio as a proxy for pulmonary arterial enlargement.³² The PAD/

AoD ratio is limited by many factors, not the least of which is the considerable variability in aortic size that is independent of PAP. However, most of the studies evaluating pulmonary arterial size (pulmonary trunk and the right and left main pulmonary arteries) in patients with PAH (and other causes of PH) on NCCT are not prospectively case controlled; very few correct for male and female sex differences, a few relate the size of these vessels to the body mass index (BMI), and no standard method has been agreed upon to measure these vessels (Table 4). Given these difficulties, it is surprising that any of these arterial measurements have shown even modest efficacy for the determination of elevated PAP.

NCCT can be definitive for the diagnosis of pulmonary veno-occlusive disease (PVOD), which is a rare but clinically important cause of PAH.⁴⁴ This disorder can occur at any age; however, it is more common in children and young adults. This is a very uncommon disease with an incidence reported to be approximately 0.1 to 0.2/10⁶ individuals. PVOD tends to have a rapid onset of symptoms with little RVH. This is one of the few causes of PAH that occurs on the "postcapillary" side of the flow of fluid through the lungs. Of the 7 patients in Frazier et al's⁴⁴ series from the Armed Forces Institute of Pathology, 6 demonstrated the following evidence for long-standing PAH on CT: (1) RV enlargement; (2) pulmonary artery > 3 cm in diameter; (3) pericardial effusion; and (4) reflux of contrast into the hepatic veins. The imaging findings on CT that can help distinguish PVOD from other more common causes of PAH include patchy ground-glass opacities, poorly defined centrilobular nodules in a random lung zonal distribution, smooth interlobular septal thickening, pleural effusions, and lymphadenopathy; these features are not typical of precapillary causes of PAH.

NCCT is also very helpful in suggesting the diagnosis of another very rare disease that can cause PAH: pulmonary capillary hemangiomatosis (PCH).⁴⁴ Up to 30% of these patients may present with hemoptysis. The CT findings of PCH are similar to those of PVOD in that there is an enlarged pulmonary trunk with a normal-sized left atrium. There are, however, some distinct differences between these 2 entities. In contrast to PVOD, there are fewer smoothly thickened interlobular septae and more ground-glass opacities that are either geographic or nodular (related to plexiform angiopathy) in PCH.

The imaging diagnosis is of critical importance for both PVOD and PCH patients. This is because if therapy with vasodilators is instituted the outcome can be fatal. The reason for this complication is interesting from a physiological point of view. With the pharmacologically induced pulmonary arterial vasodilation, a rapid pressure drop occurs in the pulmonary arteries. However, these arteries must continue to pump blood against the fixed high pressure of the pulmonary capillaries (PCH) or postcapillary venules (PVOD). This new pressure differential results in a transudate of fluid into the alveoli that can critically flood the alveolar spaces. The hallmark of both of these disorders (PCH and PVOD) is the presence of normal (or low) pulmonary capillary wedge pressure in PAH.

LIVER DISEASE MAY AFFECT THE PULMONARY CIRCULATION

There are two conditions of the pulmonary circulation that are directly related to liver disease: portopulmonary

hypertension and hepatopulmonary syndrome.^{45,46} In portopulmonary hypertension, the cause of PAH is related to excessive pulmonary arterial vasoconstriction eventually leading to cor pulmonale. Hepatic cirrhosis and the presence of portal hypertension (esophageal varices) can be important clues to the possible presence of this important complication of liver disease. The CT findings in portopulmonary hypertension are pulmonary arterial enlargement and right-sided heart dysfunction associated with liver disease. At many liver transplant centers this is a frequently undiagnosed comorbid condition in those patients awaiting liver transplantation, which can lead to rapid death. One report has shown a 50% mortality rate at 6 months in this disease.

The second condition that can be seen in this population is hepatopulmonary syndrome, which is caused by the presence of many small intrapulmonary shunts (right to left shunt as blood bypasses the alveolus) at the capillary level that results in an admixture lesion leading to peripheral hypoxemia that can be difficult to treat.⁴⁵ This entity can also be demonstrated with an echocardiographic contrast study (microbubbles in the left atrium) or a V/Q scan (^{99m}Tc-MAA in the organs). Patients with hepatopulmonary syndrome may have abnormal CT scans with vessels extending to the lung periphery without fibrosis. Secondary findings of portal venous hypertension such as ascites,

esophageal varices, and hepatic cirrhosis may also be apparent.

CTA OF ELEVATED PAP

The prototype disease for the demonstration of chronic PH is chronic pulmonary thromboembolic disease (CTEPH) (Figs. 4, 5). The diagnosis of this disease has been traditionally established with V/Q scanning and RHC. However, CTA can also be useful in the diagnosis and follow-up of these patients.^{47,48} The underlying histopathology of this disease involves the chronic deposition of thrombi and cytokine-mediated scarring leading to increase in PAP. This can be seen even after 1 episode of PE. The increased PAP induces smooth muscle cell hypertrophy of the small pulmonary arterioles. This vicious cycle repeats itself over and over again, finally leading to death from cor pulmonale.

The CTA findings of CTEPH can be divided into 3 main categories: pulmonary artery findings, other cardiovascular findings, and pulmonary parenchymal findings. The pulmonary artery findings for CTEPH include: (a) eccentric and/or circumferential thrombus that rarely calcifies; (b) intravascular webs; (c) beading of the vessels; (d) vessel truncation; (e) thready vessels; and (f) enlargement of the pulmonary trunk. The other cardiovascular findings include: (a) RVH and (b) bronchial artery hypertrophy.

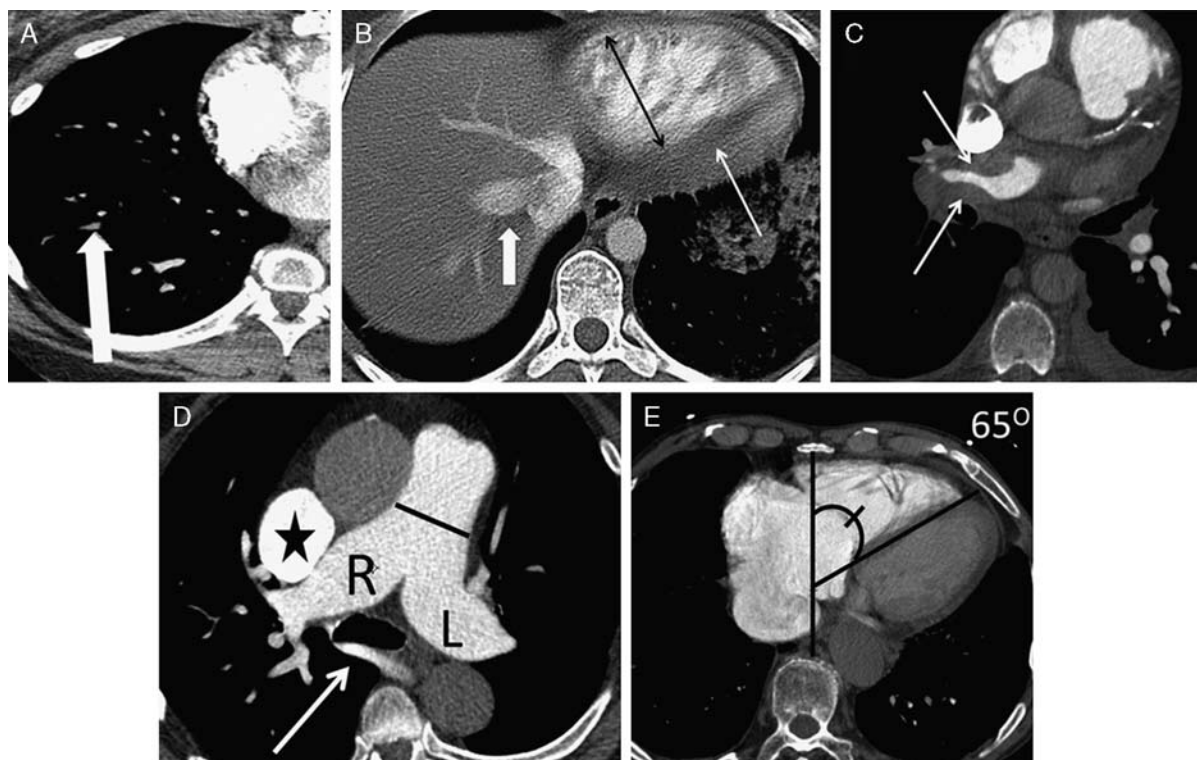


FIGURE 4. CTA findings in PH. A, CTEPH with an embolus (arrow) in a subsegmental branch of the lateral segment of the right lower lobe. B, Elevated PAP can be inferred from interventricular septal straightening (thin white arrow) and RV free wall enlargement (thin black arrow). There is reflux into the hepatic veins (thick white arrow) and inferior vena cava, which is an imaging feature of elevated central venous pressure. C, CTA from a patient with CTEPH showing circumferential chronic clot in the right main pulmonary artery (arrows). This can be removed surgically (pulmonary thromboemblectomy) with a postsurgical lowering of the mPAP. This surgery results in improved life expectancy for these patients. D, Dextro-phase CTA showing an enlargement of the SVC (star), pulmonary trunk (black line), and the right (R) and left (L) main pulmonary arteries with reflux into the azygous vein (white arrow). E, CTA of PH showing an increased ventricular septal angle at 65 degrees.

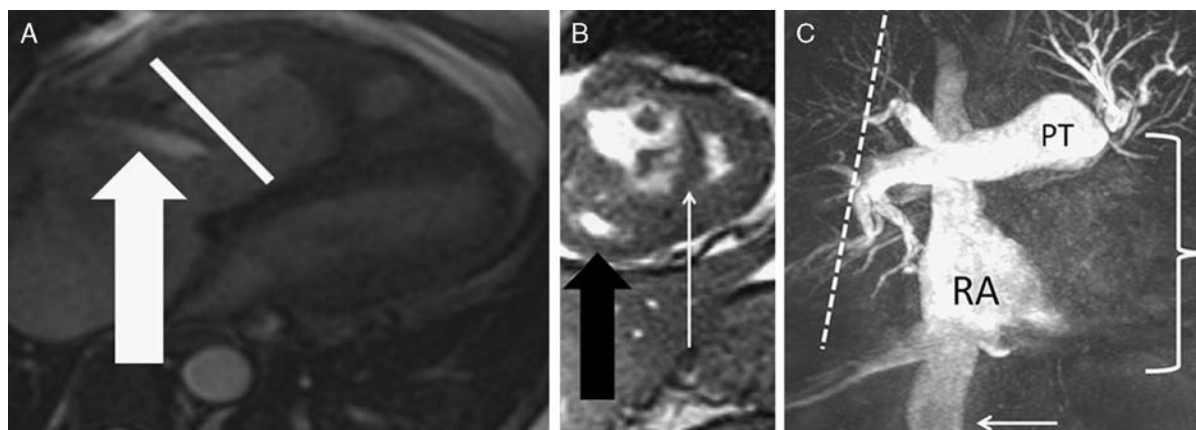


FIGURE 5. Cardiac MRI of PH. A, CTEPH 4-chamber SSFP showing a jet of TR parallel to the anterior leaflet of the tricuspid valve (arrow). The jet velocity and total flow of TR can be quantified with phase-contrast MRI using an offline workstation. The TR jet velocity is proportional to the mPAP. The short axis of the RV is increased in size (line). B, CTEPH short-axis SSFP showing RVH (black fat arrow) and bowing of the IVS (white small arrow). This bowing indicates that the pressure in the RV exceeds the pressure in the LV at that specific time point in the cardiac cycle. C, Dextro-phase MRA showing reflux into the inferior vena cava (white arrow), enlarged pulmonary trunk (PT), occlusion of left lower lobe pulmonary artery with a total lack of perfusion to the left lower lobe (bracket), and pruning of the right lung peripheral pulmonary arterial vasculature (dashed line).

The primary lung parenchymal finding is the “mosaic pattern” of decreased lung parenchymal attenuation from the chronic loss of perfusion.⁴⁹ Note that the “mosaic pattern” can be differentiated from air trapping by the use of “end-expiratory” NCCT imaging. In cases of air trapping, the “mosaic pattern” will not normalize. Another parenchymal finding includes cylindrical traction bronchiectasis, which occurs from repeated bouts of post thrombotic fibro-vascular fibrosis. This last finding (bronchiectasis) is important because a simple comparison with the vessel size can be misleading as the vessel may be small because of chronic embolic disease or simply look small, due to comparison with a larger adjacent “bronchiectatic” bronchus. The coexistence of multiple findings is usually related to CTEPH, and the patient is likely to be symptomatic.

There are other causes of bronchial arterial enlargement besides CTEPH that may be seen in chronic PH. These include the following related conditions: bronchiectasis (most notably cystic fibrosis), fibrosing mediastinitis (Dana Point 5), and congenital heart disease with Eisenmenger physiology. It can be challenging to visualize these bronchial arteries on routine transverse images; yet, they often explain hemoptysis in PH. They are often better seen on coronal images. Thin-section coronal maximum-intensity projections (MIP) (4 to 7 mm) are especially useful for visualizing bronchial arteries.

FRACTAL ANALYSIS OF VESSEL PRUNING IN PAH

The pulmonary arterial tree in patients with chronically elevated PAP shows pruning, as the central elastic pulmonary arterial vessels expand because of the La Place’s law, whereas the smaller peripheral pulmonary arteries resist pressure-induced enlargement by smooth muscle hypertrophy in their media. Recognition of this response by the pulmonary vascular bed to chronically elevated PAP can be exploited by analyzing the MIP data of the pulmonary arterial tree using a mathematical method called fractal analysis. Recently, Haitao et al⁵⁰ and colleagues

showed some utility for this approach wherein the fractal dimension (FD) for patients with PH is determined. Briefly, when using the box counting method, the FD is defined as the slope of the log of the number of boxes plotted against the log of 1/box size. In their investigation using CTA data from 14 PH patients and 17 normal individuals, the FD calculated was found to be correlated with PAP ($r = 0.82$; $P < 0.05$).⁵⁰ This method may prove to have some merit in the clinical setting as it is a mathematical construct of the patient’s pulmonary arterial branching pattern and volume, which may prove to be more useful than simple arterial size measurements. The observation of important vessel pruning may be found in any of the diseases listed in Dana Point 1 (PAH). The severity of pruning tends to be far less in Dana Point categories 2 to 5 (PH).

CTA BIOMARKERS FOR ELEVATED PAP

Currently, when CTA is used for PH assessment, a nongated PE protocol is used with images manipulated on a 3D workstation. Assessment of the RV for enlargement and hypertrophy is combined with evaluation of the lung parenchyma for diffuse disease. The pulmonary arteries are assessed for caliber and filling defects. MIPs are used to identify bronchial arteries and further evaluate any diffuse parenchymal disease. When combined (evaluation of the lung parenchyma with RV assessment), the CTA can be highly useful for characterization of the many causes of elevated PAP.

Another finding that may be appreciated on CTA for PH is calcification of an eccentric thrombus. Although this happens rarely in CTEPH, this finding is more commonly seen in other causes of PH, including mitral valve disease and Eisenmenger syndrome. Calcification of the pulmonary artery and enlargement of the RV is a sign of congenital heart disease. Eisenmenger syndrome is characterized by PH, increased pulmonary resistance, and reversal of blood flow. Care must be taken to avoid assuming that all eccentric calcified thrombi are due to CTEPH.

Wells et al⁵¹ have shown that the PAD/AoD ratio is associated with chronic obstructive pulmonary disease exacerbations, presumably because the pulmonary artery is larger in those patients with more severe PH. The use of cardiac gating with CTA is helpful, as centerline measurements, double-oblique short-axis measurements, and/or volume measurements can help to more accurately characterize the size of the pulmonary trunk and right and left main pulmonary arteries. A recent publication in patients without known pulmonary disease determined the normal end-diastolic double-oblique short-axis mean measurement for the main PAD to be 2.5 cm with a very broad range (1.89 to 3.03 cm \pm 2 SD). When this was corrected for body surface area, the mean PAD was 1.2 cm (range, 0.94 to 1.7 cm) (Table 3). The current normograms for aortic size have taken into account age, sex, and BMI. However, there are no normograms for the pulmonary trunk that take age and sex into account, nor is there an agreed-upon standard way to measure it. There are only a few publications that have indexed their PAD measurements to body surface area.^{18,19,23,52} In addition, this added measurement has not been demonstrated to improve the accuracy of CTA for PH detection.⁵³ One benefit of CTA is that it reliably allows for comparison of the segmental and lobar arteries with their corresponding bronchi. The bronchi cannot be reliably measured on MRI, although the use of ultrashort time to echo shows some promise for the visualization of lung structure.⁵⁴ Studies have shown that the degree of enlargement of the segmental artery/bronchus ratio corresponds to the severity of PH and is highly reproducible.⁵³ Gated studies may have a role in the assessment of RV volumes when the patient is unable to undergo MRI. This use of CTA for the calculation of RV or LV function is often limited in clinical settings because of concerns pertaining to medical radiation from acquisition of both end-systolic and end-diastolic phases. This limitation may not be as important an issue in the future, as dose reduction methods are being explored more comprehensively for this purpose.

THE SEPTAL ANGLE IS INCREASED IN PATIENTS WITH ELEVATED PAP

The use of cardiac gating has allowed investigators to determine RV functional parameters from CTA. At present, in most cases, CTA for the evaluation of PH is not performed with electrocardiography (EKG) gating. This method, however, does rely on retrospective gating, which increases the radiation dose; thus, this method has some important drawbacks. Liu et al⁵⁵ have recently demonstrated the efficacy of using the septal angle as a CTA-derived parameter of the position of the IVS in relation to the anterior posterior axis determined by the mid sternum and mid vertebral body at the level of the IVS (Fig. 4). They found that the septal angle in patients with CTEPH correlated with PVR ($P < 0.001$).

LIMITED STANDARDIZATION OF CTA MEASUREMENTS IN PAH IS A PROBLEM

The specialties of thoracic radiology and pulmonary medicine can be advanced by reaching a consensus on how to measure the pulmonary artery. Similar to the extensive literature that is now available for the ascending aorta and its propensity for aortic dissection based on size, our specialty could create normograms of the pulmonary artery that take the following features into account: (1) cardiac

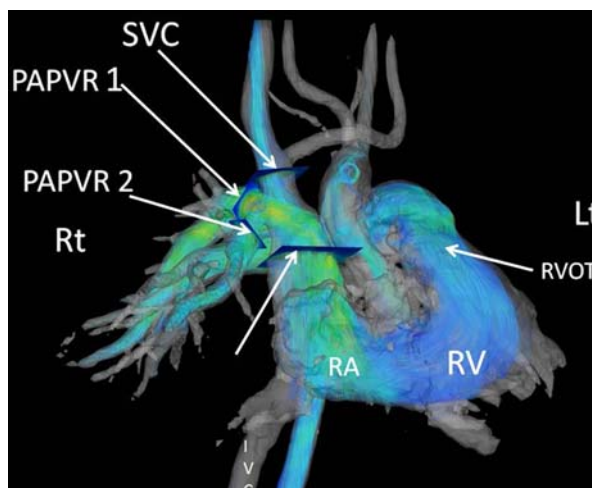


FIGURE 6. 4D flow MRI of PAH from partial anomalous pulmonary venous return (Dana Point 1.4.4). Images were postprocessed from a respiratory gated phase contrast vastly undersampled isotropic projection reconstruction (PC-VIPR). These streamlines are color coded for velocity information. The individual contributions of each anomalous vein can be derived from an offline workstation with tools that convert the phase shift information to flow over the cardiac cycle for each manually selected cut plane. The separate cut planes for the SVC and the 2 anomalous pulmonary veins (PAPVR1 and PAPVR2) are shown by arrows. (Postprocessing using Encyte performed by Phillip Kilgas and Elizabeth Nett, PhD.) IVC indicates inferior vena cava; Lt, left; RA, right atrium; Rt, right; RVOT, RV outflow tract.

phase, (2) sex, (3) age, and (4) index to BMI for all chest examinations. It is likely that these precisely defined and indexed measurements of the pulmonary artery would have a better correlation with elevated pulmonary pressure and be predictive of early death from this disease.

ECHOCARDIOGRAPHY REMAINS THE NONINVASIVE TEST OF CHOICE FOR ELEVATED PAP

Despite the many advantages of MRI, echocardiography still remains the examination of choice for PAH (and other causes of PH) diagnosis and follow-up before RHC. This fact may be related to the convenience of echocardiography, as it can be performed at the bedside on very sick patients.³⁹

MRI OF ELEVATED PAP

Of all the noninvasive methods now available for the diagnosis and follow-up of patients with PAH, and other causes of PH, MRI is the most popular (Figs. 6, 7). The use of MRI in the setting of known or suspected PH can be a helpful adjunct to the currently available tests [RHC, TTE, transesophageal echocardiography, V/Q scanning, and pulmonary function tests] because of its highly accurate and reproducible analysis of RV ejection fraction (RVEF) (Table 4).^{27–31} MRI and MRA are more accurate for the morphologic assessment of RV morphology and function, and have better reproducibility for the determination of ventricular mass, RVEF, RV stroke volume (RVSV), RVEDV, RVEDV_{index}, right and left atrial size, regurgitant jet velocity and volume, myocardial scarring, flow patterns of interventricular bulk flow, pulmonary venous anatomy,

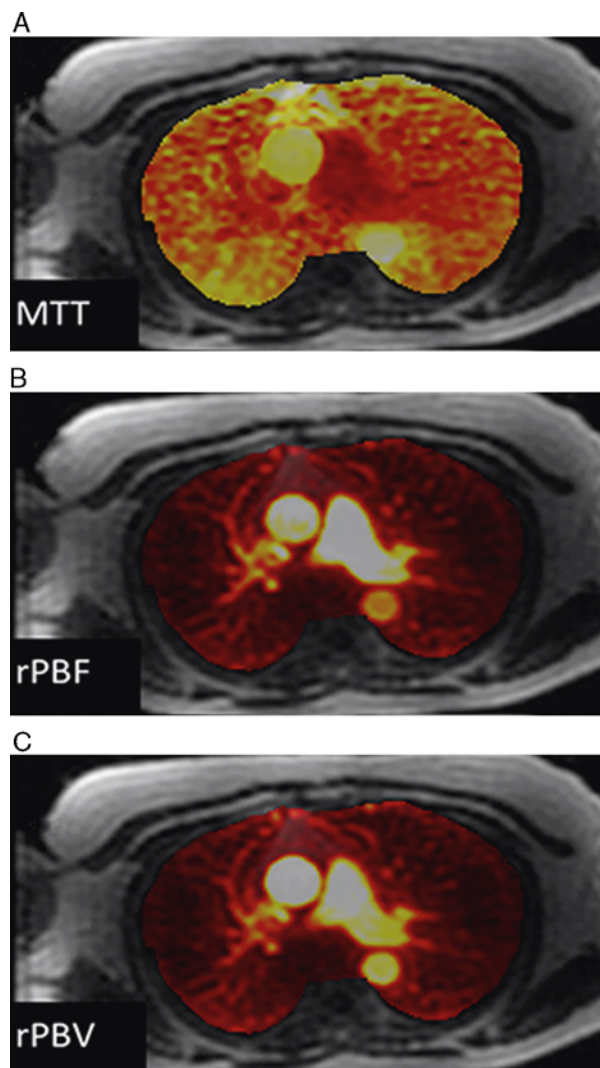


FIGURE 7. Pulmonary perfusion in a normal volunteer (images were not corrected for the AIF): (A) approximate MTT; (B) relative pulmonary blood flow (rPBF); (C) relative PBV (rPBV). Images courtesy of Scott Nagle, MD, PhD, and Laura Bell, MS.

LV stroke volume, ventricular end-diastolic volume (LVEDV), LVEDV_{index}, and LV systolic volume index.^{56,57}

SURVIVAL IN PATIENTS WITH ELEVATED PAP IS DIRECTLY RELATED TO RV FUNCTION

As recently shown by van de Veerdonk et al²⁸ in patients undergoing medical therapy for PAH, an improvement in RVEF was found to be highly correlated with survival ($P < 0.014$), whereas changes in PVR were not ($P < 0.8$) (Table 4). These authors concluded that if the RV does not recover function with medical therapy, despite the lowering of mPAP, the inevitable cascade of events leading to early death from cor pulmonale will occur.²⁸

The quantitative aspects of MRI are becoming more important for the study of patients with elevated PAP, as these measurements can provide noninvasive biomarkers for this disease that may facilitate surgical management or medical treatment decisions.^{19,58–60} The various parameters

that can be quantified by MRI are: (1) morphologic—measurement of chamber and vessel size throughout the cardiac cycle for RV and LV ejection fractions, ventricular mass, and end-diastolic and end-systolic mass indices; (2) measurement of flow throughout the cardiac cycle (velocity, direction, and acceleration), which is very helpful for the quantification of (a) tricuspid valve regurgitation and/or pulmonic regurgitation, (b) early “e” and late “a” atrial wave net flows into the right atrium, (c) vessel wall compliance, and (d) wall shear stress.

MRI IN CTEPH

In patients with CTEPH, MRA is similar to CTA in terms of revealing the details of the central pulmonary arteries; it can also show subsegmental vessels using parallel imaging and breath-holding techniques (Fig. 5).^{58,61} Survival in patients with PH from CTEPH is better when RVEF is preserved, whereas the combination of elevated mPAP and diminished RVEF portends a very poor prognosis.²⁹ It has recently been shown that delayed contrast enhancement at the septal insertions of the myocardium is common in patients with elevated PAP.⁶⁰ The severity of PAP was found to be the primary determinant of this finding.⁶⁰ As is commonly seen on TTE and/or transesophageal echocardiography, the presence of systemic (or greater) RV pressure/volume overload is shown on cine MRI on short-axis imaging by observing the bowing of the IVS toward the LV.^{56,62} The shift in the position of the IVS from convex to concave is directly proportional to the mPAP and PVR. The reason for this bowing in the setting of congenital heart disease with a right to left shunt can be related to the PAP being greater than systemic such as is found in the Eisenmenger syndrome. In the acute setting of elevated PAP due to pulmonary embolus, the RV cannot generate systemic pressures > 40 mm Hg, and in the chronic state the mPAP is often still lower than systemic pressure; thus, another explanation is needed for septal bowing. This finding represents a change in the ventricular coupling. The concept of IVS bowing in both acute and chronic elevation of PAP is explained by mechanical asynchrony (uncoupling) wherein the elongation of the RV contraction and underfilled LV concert to allow for bowing from right to left of the IVS.⁶²

COMBINING STRUCTURAL AND FUNCTIONAL ANALYSIS IMPROVES EFFICACY FOR MRI CTEPH

MRI has an evolving role in the workup of CTEPH. Using CTA as the gold standard, the active PH group in Sheffield, United Kingdom, has recently shown that by combining noncontrast MRI (proton density), MRA, and perfusion MRA, an improvement can be seen in the ability to diagnose CTEPH over the use of MRA images alone.⁶³ Using CTA as the gold standard in their study on 53 CTEPH patients (and 36 controls), they found that MRA showed excellent results for the diagnosis of this disorder (98% sensitivity and 94% specificity). Each patient underwent 3 MRI series: (1) precontrast SSFP acquisition; (2) time-resolved contrast-enhanced (CE) MRA (TRICKS); and (3) high-resolution CE-MRA. The CE-MRA alone showed 92% sensitivity for the diagnosis of chronic thromboembolism.⁶¹ For the centrally based disease of chronic clot in the main pulmonary arteries, use of SSFP images was very helpful. Of interest was the fact that the CE-MRA was able to detect disease with greater frequency compared with the CTA in the

following situations: stenosis, 29/18; poststenotic dilation, 23/7; and occlusions 37/29.⁶¹ These areas of better performance are not well demonstrated using the statistical method that assumes CTA as the gold standard. Thus, MRA would appear to underperform CTA from the point of view of simple sensitivity and specificity, when in fact it has performed better. As could be expected, CTA was better at determining the presence of (a) webs and bands from resolving clot and (b) adherent wall thrombi. Analysis of the lung parenchyma for nodules or evidence of PCH or PVOD is also a known weakness of MRA. The authors did not address the issue of how well mosaic perfusion was detected by the time-resolved MRA compared with CTA in their patients with CTEPH.

MR MEASUREMENT OF SHUNT FRACTION (Qp/Qs)

The calculation of shunt fractions (Qp/Qs) in patients with congenital heart disease is an important application of MRA phase-contrast flow methodology.⁶⁴ The shunt fraction and how it changes over the lifetime of the patient can be monitored noninvasively. Of note, however, is the fact that, unlike RHC, oxygen saturation in the chambers of the heart cannot be measured using MRI. Typically, patients with left to right shunts will be considered for operative management when the shunt fraction (Qp/Qs) is > 1.5.

MR MEASUREMENT OF TR AND PULMONIC VALVULAR REGURGITATION

For the quantification of valvular regurgitation standard SSFP images are not as useful as echocardiography or phase-contrast methods for the detection of mild regurgitant jets.⁶⁵ The regurgitant fraction for each valve can be determined, which is a major advantage of phase contrast MRI.⁶⁵ The issue of estimating the mPAP from the TR jet velocity using phase contrast MRI is not that the jet velocity cannot be measured, as much as it is reflective of the fact that the modified Bernoulli equation itself has limitations.

NONCONTRAST PERFUSION AND VENTILATION MRI

The use of noncontrast Fourier decomposition has been recently introduced as a new method for visualizing lung ventilation and perfusion.^{66,67} Although this method is not currently ready for clinical use, it offers the following benefits for future research in pulmonary functional imaging: (a) no requirement for intravenous contrast; (b) no requirement for inhaled contrast; (c) no radiation required; and (d) no breath-holding required. The pulse uses a 2D balanced SSFP pulse sequence to acquire a few coronal (typically 4 to 6) 2D images of the chest at a temporal resolution of 3 to 4 frames/s. The data are processed to separate the contributions of respiratory motion (ventilation) and cardiac pulsatility (perfusion) to the observed signal changes on a pixel-by-pixel basis. This postprocessing first involves the use of nonrigid image registration to remove bulk motion from the time series of images, followed by time-domain Fourier analysis, taking advantage of the fact that the frequency of respiratory motion is different from that of cardiac pulsatility. This method is in the validation stage now; however, given its safety profile and low cost, this holds promise for the future of functional lung imaging.

4D FLOW ALLOWS FOR VOLUMETRIC SAMPLING OF PHASE-CONTRAST INFORMATION

A new MRA method for the quantification of flow, called "4D flow" imaging, has been introduced recently (Fig. 6). This method has velocity encoding that can be either prospectively or retrospectively cardiac gated and is volumetric. It allows for multidirectional flow visualization with either particle traces or stream lines in the heart and large vessels (Fig. 4C).^{68–70} However, this is only made possible after extensive postprocessing using advanced visualization tools on a workstation using data from a respiratory and cardiac-gated, volumetric, phase-contrast acquisition at a defined amount of velocity encoding using a non-Cartesian reconstruction of the k-space data. This is a promising new visualization technique that may have some utility for pulmonary arterial flow analysis within the larger pulmonary arteries in patients with PAH.⁵⁶ Reiter et al⁷¹ found that normal individuals demonstrate flow toward the distal pulmonary arteries throughout the cardiac cycle. In those patients with both early (latent) and known PAH, flow vortices directed in a retrograde manner were identified in the main pulmonary artery.⁷¹ The time period during which these vortices existed directly correlated with the mPAP at rest ($r = 0.94$; 95% CI, 0.85–0.97).⁷¹ This is a quantitative visualization method by which one is able to determine what exactly happens to the RVSV, which is known to have an increased residence time in the proximal pulmonary arterial circuit because of increased PVR.

MR MEASUREMENT OF DIMINISHED PULMONARY PERFUSION IN PAH

MRI perfusion methods have been used successfully in PH patients demonstrating, as could be suspected, a delayed transit time in patients compared with normal individuals (Fig. 7).^{57,72} Calculation of perfusion parameters, including mean transit time (MTT), time to peak, and blood volume (PBV), can in theory be performed using a well-established methodology based on the indicator dilution theory⁷³ and the following formulas:

$$C_{VOI}(t) = \text{PBF} \int_0^t C_{AIF}(\tau) \times R(t-\tau) d\tau, \quad (1)$$

$$\text{PBV} = \frac{\int_0^\infty C_{VOI}(t) dt}{\int_0^\infty C_{AIF}(t) dt}, \quad (2)$$

$$\text{MTT} = \frac{\text{PBV}}{\text{PBF}}, \quad (3)$$

where $C_{VOI}(t)$ is the contrast agent concentration in the volume of interest, $C_{AIF}(t)$ is the contrast agent concentration in the pulmonary artery (arterial input function: AIF), and $R(t)$ is the fraction of contrast agent remaining at time (t). However, these calculations require postprocessing on a workstation that is not routinely available to most imagers. As can be seen, all of these derived values are critically dependent on first obtaining the AIF, which is typically obtained by measuring the signal intensity as a function of time in the pulmonary trunk.⁷²

Ley et al⁵⁷ evaluated 20 patients with PH and 5 normal volunteers and determined the MTT, time to peak, and PBV (Fig. 6) using a 3D FLASH method after infusion of 0.1 mmol Gd-DTPA/kg. They found that, for the variables

measured, only the dorsal transit times showed any significant difference between the PH patients and normal individuals ($P = 0.04$).⁵⁷

Perfusion of the lung is influenced by the presence and severity of PAH. This can be demonstrated using a 3D MRA first-pass CE-MRA perfusion image. As shown by Ohno et al⁷² there was significant difference in MTT and PBV between patients with PAH and normal patients.⁷² The normal patients in their study had almost twice the blood flow (13 vs. 7 L/min) and a more rapid (shorter) MTT (5 vs. 8 s) compared with patients with PAH.⁷²

There remain some important problems with quantitative pulmonary perfusion MRI. Most importantly, unlike iodinated contrast agents, in which concentration scales linearly and can be directly measured using CT Hounsfield units, the MR signal intensity of gadolinium-based contrast agents (GBCAs) scales as a nonlinear function of GBCA concentration, and therefore cannot be measured directly on MR images. Therefore, the measured signal intensity from a single MRA voxel (VOI) does not convert to an absolute concentration of Gadolinium based contrast agents. At high contrast concentrations (such as those often seen in the pulmonary artery), saturation effects can blunt the measured AIF, causing underestimation of the contrast concentration at higher concentrations. This problem can result in an erroneous AIF profile. Simply decreasing the administered contrast dose can decrease these errors in determining the AIF. However, this results in very low lung tissue signal to noise ratio, making the perfusion parameter calculations (performed at low dose) very sensitive to noise. Two strategies have been used to mitigate these problems: (1) a low-dose method⁷⁴; and (2) a dual-bolus method.⁷⁵ An additional, often overlooked, source of error in reported “quantitative” MRI perfusion measurements is the lack of correction for the patient’s hematocrit level in all pulmonary blood flow calculations. Blood plasma is known to flow more slowly than erythrocytes in the blood.⁷⁶ As gadolinium is principally dissolved in plasma, raw uncorrected flow measures are more related to plasma flow than to the more physiologically important, and faster, erythrocyte flow. There are known methods for correcting this difference⁷³; however, these require measurement of hematocrit in the pulmonary vasculature, which can differ from the measures of peripheral venous hematocrit. The picture becomes even more complex when one considers that each GBCA has a unique amount of albumin binding, and many GBCAs are not strictly intravascular. Suffice it to say that, although great progress has been made toward quantitative pulmonary perfusion, significant work remains to be done.

PULMONARY ARTERIAL COMPLIANCE DECREASES IN PH

Pulmonary arterial compliance in the large elastic vessels of the proximal pulmonary arterial tree diminishes with chronically elevated PAP. First described by Otto Frank in 1899, the “Windkessel” is a heuristic device wherein the effect of varying arterial compliance can be modeled mathematically (lumped model) to help explain how changes in elasticity of large vessels affect blood pressure and the pulse wave velocity.^{63,77,78} This loss of elasticity (stiffening) coupled with increased PVR is problematic for RV function.⁷⁷ This change results in an increased afterload on the RV as it has no easy reservoir (pressure relief) to deliver its stroke volume to and must pump directly against the increase PVR of the

hypertrophied muscular arterial system of the branch pulmonary arteries. Stated in another way, chronic PAH robs the right heart of this natural reservoir (compliant/elastic pulmonary arteries) to store the energy (pressure) and volume delivered (flow) to the proximal pulmonary arteries. The lack of this energy storage (in the now noncompliant pulmonary arterial system) weakens the RV by forcing it to hypertrophy in the face of increasing afterload of the pulmonary circulation.

One interesting feature of MRI is its ability to help quantify pulmonary artery stiffness when combined with RHC.⁷⁹ In animal models of PH, pulmonary arterial wall stiffness has been shown to increase with PH progression.⁸⁰ Clinically, pulmonary artery stiffness, and its noninvasively measured surrogate, the RAC (RAC = maximum systolic area – minimum diastolic area/maximum systolic area), have been shown to be independent predictors of mortality in PAH.³¹ Recently, in a canine model of acute PH, both the arterial stiffness coefficient β [$\beta = \ln(\text{systolic PAP}/\text{diastolic PAP}/2\text{RAC})$] and the RAC were found to correlate with the overall pulmonary vascular compliance measured as the ratio of stroke volume to pulse pressure.⁷⁹ Stiffness of the pulmonary arterial system has many important implications for the RV; in particular, the afterload of the RV is increased from the oscillatory work of the RV because of the lack of compliance in both the proximal and distal pulmonary arteries. Several indexes of pulmonary artery stiffness can be calculated in humans (elasticity, distensibility, capacitance, stiffness constant (β), and pulse pressure) from combined RHC and MRI data.⁸⁰ Stevens and colleagues recently demonstrated that elevated PA stiffness was associated with lower RVEF, greater RVH, and dilation. In addition, and more importantly, alterations in PA elasticity appear to have occurred earlier than RV performance changes.⁸⁰

SUMMARY

This has been a review of how the known structural and functional changes associated with elevated PAP (PAH and PH) can be studied with MRI and CT. By understanding the dynamic relationship that exists between the heart and the lungs in this heterogeneous group of diseases, the severity of this disease process can often be inferred. MRI is a promising noninvasive and nonionizing modality that can be used to study the many diseases that cause PAH and PH in a longitudinal manner. In the future, this method can be used to sequentially track the many parameters proven to have a direct relationship with survival: RAC of the pulmonary trunk, RVS_{index}, RVS_V, RVEDV_{index}, LVEDV_{index}, and baseline RVEF < 35%. This may allow for a better degree of personalization of the treatment regimen without having to resort to repeated RHCs for the longitudinal assessment of those unfortunate patients valiantly struggling to survive with this relentlessly progressive disease.

REFERENCES

1. Humbert M. The burden of pulmonary hypertension. *Eur Respir J*. 2007;30:1–2.
2. Strange G, Playford D, Stewart S, et al. Pulmonary hypertension: prevalence and mortality in the Armadale echocardiography cohort. *Heart*. 2012;98:1805–1811.
3. Simonneau G, Robbins IM, Beghetti M, et al. Updated clinical classification of pulmonary hypertension. *J Am Coll Cardiol*. 2009;54(suppl):S43–S54.
4. Galie N, Hoeper MM, Humbert M, et al. Guidelines for the diagnosis and treatment of pulmonary hypertension: the Task

- Force for the Diagnosis and Treatment of Pulmonary Hypertension of the European Society of Cardiology (ESC) and the European Respiratory Society (ERS), endorsed by the International Society of Heart and Lung Transplantation (ISHLT). *Eur Heart J*. 2009;30:2493–2537.
5. Chin KM, Kim NH, Rubin LJ. The right ventricle in pulmonary hypertension. *Coron Artery Dis*. 2005;16:13–18.
 6. Humbert M, Sitbon O, Chaouat A, et al. Pulmonary arterial hypertension in France: results from a national registry. *Am J Respir Crit Care Med*. 2006;173:1023–1030.
 7. Rich S, Dantzker DR, Ayres SM, et al. Primary pulmonary hypertension. A national prospective study. *Ann Intern Med*. 1987;107:216–223.
 8. Badesch DB, Raskob GE, Elliott CG, et al. Pulmonary arterial hypertension: baseline characteristics from the REVEAL Registry. *Chest*. 2010;137:376–387.
 9. Thenappan T, Shah SJ, Rich S, et al. USA-based registry for pulmonary arterial hypertension: 1982–2006. *Eur Respir J*. 2007;30:1103–1110.
 10. Peacock AJ, Murphy NF, McMurray JJ, et al. An epidemiological study of pulmonary arterial hypertension. *Eur Respir J*. 2007;30:104–109.
 11. Hyduk A, Croft JB, Ayala C, et al. Pulmonary hypertension surveillance—United States, 1980–2002. *MMWR Surveill Summ*. 2005;54:1–28.
 12. D'Alonzo GE, Barst RJ, Ayres SM, et al. Survival in patients with primary pulmonary hypertension. Results from a national prospective registry. *Ann Intern Med*. 1991;115:343–349.
 13. Hui-li G. The management of acute pulmonary arterial hypertension. *Cardiovasc Ther*. 2011;29:153–175.
 14. van Beek EJ, Kuijper PM, Buller HR, et al. The clinical course of patients with suspected pulmonary embolism. *Arch Intern Med*. 1997;157:2593–2598.
 15. Goodman LR, Lipchik RJ, Kuzo RS, et al. Subsequent pulmonary embolism: risk after a negative helical CT pulmonary angiogram—prospective comparison with scintigraphy. *Radiology*. 2000;215:535–542.
 16. Qanadli SD, El Hajjam M, Vieillard-Baron A, et al. New CT index to quantify arterial obstruction in pulmonary embolism: comparison with angiographic index and echocardiography. *Am J Roentgenol*. 2001;176:1415–1420.
 17. Kuriyama K, Gamsu G, Stern RG, et al. CT-determined pulmonary artery diameters in predicting pulmonary hypertension. *Invest Radiol*. 1984;19:16–22.
 18. Frank H, Globits S, Glogar D, et al. Detection and quantification of pulmonary artery hypertension with MR imaging: results in 23 patients. *Am J Roentgenol*. 1993;161:27–31.
 19. Murray TI, Boxt LM, Katz J, et al. Estimation of pulmonary artery pressure in patients with primary pulmonary hypertension by quantitative analysis of magnetic resonance images. *J Thorac Imaging*. 1994;9:198–204.
 20. Edwards PD, Bull RK, Coulden R. CT measurement of main pulmonary artery diameter. *Br J Radiol*. 1998;71:1018–1020.
 21. Sanal S, Aronow WS, Ravipati G, et al. Prediction of moderate or severe pulmonary hypertension by main pulmonary artery diameter and main pulmonary artery diameter/ascending aorta diameter in pulmonary embolism. *Cardiol Rev*. 2006;14:213–214.
 22. Beiderlinden M, Kuehl H, Boes T, et al. Prevalence of pulmonary hypertension associated with severe acute respiratory distress syndrome: predictive value of computed tomography. *Intensive Care Med*. 2006;32:852–857.
 23. Zisman DA, Karlamangla AS, Ross DJ, et al. High-resolution chest CT findings do not predict the presence of pulmonary hypertension in advanced idiopathic pulmonary fibrosis. *Chest*. 2007;132:773–779.
 24. Ghanem MK, Makhoulouf HA, Agmy GR, et al. Evaluation of recently validated non-invasive formula using basic lung functions as new screening tool for pulmonary hypertension in idiopathic pulmonary fibrosis patients. *Ann Thorac Med*. 2009;4:187–196.
 25. Linguraru MG, Pura JA, Van Uiter RL, et al. Segmentation and quantification of pulmonary artery for noninvasive CT assessment of sickle cell secondary pulmonary hypertension. *Med Phys*. 2010;37:1522–1532.
 26. Tan RT, Kuzo R, Goodman LR, et al. Utility of CT scan evaluation for predicting pulmonary hypertension in patients with parenchymal lung disease. Medical College of Wisconsin Lung Transplant Group. *Chest*. 1998;113:1250–1256.
 27. Heyer CM, Lemburg SP, Knoop H, et al. Multidetector-CT angiography in pulmonary embolism—can image parameters predict clinical outcome? *Eur Radiol*. 2011;21:1928–1937.
 28. van de Veerdonk MC, Kind T, Marcus JT, et al. Progressive right ventricular dysfunction in patients with pulmonary arterial hypertension responding to therapy. *J Am Coll Cardiol*. 2011;58:2511–2519.
 29. van Wolferen SA, Marcus JT, Boonstra A, et al. Prognostic value of right ventricular mass, volume, and function in idiopathic pulmonary arterial hypertension. *Eur Heart J*. 2007;28:1250–1257.
 30. Mathai SC, Sibley CT, Forfia PR, et al. Tricuspid annular plane systolic excursion is a robust outcome measure in systemic sclerosis-associated pulmonary arterial hypertension. *J Rheumatol*. 2011;38:2410–2418.
 31. Gan CT, Lankhaar JW, Westerhof N, et al. Noninvasively assessed pulmonary artery stiffness predicts mortality in pulmonary arterial hypertension. *Chest*. 2007;132:1906–1912.
 32. Ng CS, Wells AU, Padley SPA. CT sign of chronic pulmonary arterial hypertension: the ratio of main pulmonary artery to aortic diameter. *J Thorac Imaging*. 1999;14:270–278.
 33. Stein PD, Chenevert TL, Fowler SE, et al. Gadolinium-enhanced magnetic resonance angiography for pulmonary embolism: a multicenter prospective study (PIOPED III). *Ann Intern Med*. 2010;152:434–443, W142–W433.
 34. Revel MP, Sanchez O, Couchon S, et al. Diagnostic accuracy of magnetic resonance imaging for an acute pulmonary embolism: results of the 'IRM-EP' study. *J Thromb Haemost*. 2012;10:743–750.
 35. Kalb B, Sharma P, Tigges S, et al. MR imaging of pulmonary embolism: diagnostic accuracy of contrast-enhanced 3D MR pulmonary angiography, contrast-enhanced low-flip angle 3D GRE, and nonenhanced free-induction FISP sequences. *Radiology*. 2012;263:271–278.
 36. Schiebler ML, Nagle SK, Francois CJ, et al. Effectiveness of MR angiography for the primary diagnosis of acute pulmonary embolism: clinical outcomes at 3 months and 1 year. *J Magn Reson Imaging*. 2013. (In press) (DOI 10.1002/jmri.24057).
 37. Carrier M, Righini M, Wells PS, et al. Subsegmental pulmonary embolism diagnosed by computed tomography: incidence and clinical implications. A systematic review and meta-analysis of the management outcome studies. *J Thromb Haemost*. 2010;8:1716–1722.
 38. Pijpe A, Andrieu N, Easton DF, et al. Exposure to diagnostic radiation and risk of breast cancer among carriers of BRCA1/2 mutations: retrospective cohort study (GENE-RAD-RISK). *BMJ*. 2012;345:e5660.
 39. Sagar R, Sitbon O. Hemodynamics in pulmonary arterial hypertension: current and future perspectives. *Am J Cardiol*. 2012;110(suppl):S9–S15.
 40. Sosland RP, Gupta K. Images in cardiovascular medicine: McConnell's sign. *Circulation*. 2008;118:e517–e518.
 41. Benza RL, Miller DP, Gomberg-Maitland M, et al. Predicting survival in pulmonary arterial hypertension: insights from the Registry to Evaluate Early and Long-Term Pulmonary Arterial Hypertension Disease Management (REVEAL). *Circulation*. 2010;122:164–172.
 42. Cho EJ, Jiamsripong P, Calleja AM, et al. Right ventricular free wall circumferential strain reflects graded elevation in acute right ventricular afterload. *Am J Physiol Heart Circ Physiol*. 2009;296:H413–H420.
 43. Devaraj A, Wells AU, Meister MG, et al. Pulmonary hypertension in patients with bronchiectasis: prognostic significance of CT signs. *Am J Roentgenol*. 2011;196:1300–1304.

44. Frazier AA, Franks TJ, Mohammed TL, et al. From the archives of the AFIP: pulmonary veno-occlusive disease and pulmonary capillary hemangiomatosis. *Radiographics*. 2007; 27:867–882.
45. McAdams HP, Erasmus J, Crockett R, et al. The hepatopulmonary syndrome: radiologic findings in 10 patients. *Am J Roentgenol*. 1996;166:1379–1385.
46. Porres-Aguilar M, Altamirano JT, Torre-Delgadillo A, et al. Portopulmonary hypertension and hepatopulmonary syndrome: a clinician-oriented overview. *Eur Respir Rev*. 2012;21:223–233.
47. Darteville P, Fadel E, Mussot S, et al. Chronic thromboembolic pulmonary hypertension. *Eur Respir J*. 2004;23:637–648.
48. Willemink MJ, van Es HW, Koobs L, et al. CT evaluation of chronic thromboembolic pulmonary hypertension. *Clin Radiol*. 2012;67:277–285.
49. Rossi A, Attina D, Borgonovi A, et al. Evaluation of mosaic pattern areas in HRCT with Min-IP reconstructions in patients with pulmonary hypertension: could this evaluation replace lung perfusion scintigraphy? *Eur J Radiol*. 2012;81:e1–e6.
50. Haitao S, Ning L, Lijun G, et al. Fractal dimension analysis of MDCT images for quantifying the morphological changes of the pulmonary artery tree in patients with pulmonary hypertension. *Korean J Radiol*. 2011;12:289–296.
51. Wells JM, Washko GR, Han MK, et al. Pulmonary arterial enlargement and acute exacerbations of COPD. *N Engl J Med*. 2012;367:913–921.
52. Lin FY, Devereux RB, Roman MJ, et al. The right sided great vessels by cardiac multidetector computed tomography: normative reference values among healthy adults free of cardiopulmonary disease, hypertension, and obesity. *Acad Radiol*. 2009;16:981–987.
53. Devaraj A, Wells AU, Meister MG, et al. Detection of pulmonary hypertension with multidetector CT and echocardiography alone and in combination. *Radiology*. 2010;254: 609–616.
54. Johnson KM, Fain SB, Schiebler ML, et al. Optimized 3D ultrashort echo time pulmonary MRI. *Magn Reson Med*. 2012. doi: 10.1002/mrm.24570.
55. Liu M, Ma ZH, Guo XJ, et al. A septal angle measured on computed tomographic pulmonary angiography can non-invasively estimate pulmonary vascular resistance in patients with chronic thromboembolic pulmonary hypertension. *J Thorac Imaging*. 2012;27:325–330.
56. Bradlow WM, Gibbs JS, Mohiaddin RH. Cardiovascular magnetic resonance in pulmonary hypertension. *J Cardiovasc Magn Res*. 2012;14:1–12.
57. Ley S, Mereles D, Risse F, et al. Quantitative 3D pulmonary MR-perfusion in patients with pulmonary arterial hypertension: correlation with invasive pressure measurements. *Eur J Radiol*. 2007;61:251–255.
58. Oberholzer K, Romanekhsen B, Kunz P, et al. Contrast-enhanced 3D MR angiography of the pulmonary arteries with integrated parallel acquisition technique (iPAT) in patients with chronic-thromboembolic pulmonary hypertension CTEPH - sagittal or coronal acquisition? *RoFo Fortschr Geb Rontgenstr Nuklearmedizin*. 2004;176:605–609.
59. Ghio S, Gavazzi A, Campana C, et al. Independent and additive prognostic value of right ventricular systolic function and pulmonary artery pressure in patients with chronic heart failure. *J Am Coll Cardiol*. 2001;37:183–188.
60. Sanz J, Dellegrottaglie S, Kariisa M, et al. Prevalence and correlates of septal delayed contrast enhancement in patients with pulmonary hypertension. *Am J Cardiol*. 2007;100: 731–735.
61. Rajaram S, Swift AJ, Capener D, et al. Diagnostic accuracy of contrast-enhanced MR angiography and unenhanced proton MR imaging compared with CT pulmonary angiography in chronic thromboembolic pulmonary hypertension. *Eur Radiol*. 2012;22:310–317.
62. Marcus JT, Gan CT, Zwanenburg JJ, et al. Interventricular mechanical asynchrony in pulmonary arterial hypertension: left-to-right delay in peak shortening is related to right ventricular overload and left ventricular underfilling. *J Am Coll Cardiol*. 2008;51:750–757.
63. Frank O. The basic shape of the arterial pulse. First treatise: mathematical analysis. 1899. *J Mol Cell Cardiol*. 1990;22: 255–277.
64. Debl K, Djavidani B, Buchner S, et al. Quantification of left-to-right shunting in adult congenital heart disease: phase-contrast cine MRI compared with invasive oximetry. *Br J Radiol*. 2009;82:386–391.
65. Sommer G, Bremerich J, Lund G. Magnetic resonance imaging in valvular heart disease: clinical application and current role for patient management. *J Magn Res Imaging*. 2012;35: 1241–1252.
66. Lederlin M, Bauman G, Eichinger M, et al. Functional MRI using Fourier decomposition of lung signal: reproducibility of ventilation- and perfusion-weighted imaging in healthy volunteers. *Eur J Radiol*. 2013; PMID:23295084.
67. Bauman G, Scholz A, Rivoire J, et al. Lung ventilation- and perfusion-weighted Fourier decomposition magnetic resonance imaging: in vivo validation with hyperpolarized (³He) and dynamic contrast-enhanced MRI. *Magn Res Med*. 2013; 69:229–237.
68. Kilner PJ, Yang GZ, Mohiaddin RH, et al. Helical and retrograde secondary flow patterns in the aortic arch studied by three-directional magnetic resonance velocity mapping. *Circulation*. 1993;88(pt 1):2235–2247.
69. Kilner PJ, Yang GZ, Wilkes AJ, et al. Asymmetric redirection of flow through the heart. *Nature*. 2000;404:759–761.
70. Markl M, Kilner PJ, Ebbers T. Comprehensive 4D velocity mapping of the heart and great vessels by cardiovascular magnetic resonance. *J Cardiovasc Magn Res*. 2011;13:1–22.
71. Reiter G, Reiter U, Kovacs G, et al. Magnetic resonance-derived 3-dimensional blood flow patterns in the main pulmonary artery as a marker of pulmonary hypertension and a measure of elevated mean pulmonary arterial pressure. *Circ Cardiovasc Imaging*. 2008;1:23–30.
72. Ohno Y, Hatabu H, Murase K, et al. Primary pulmonary hypertension: 3D dynamic perfusion MRI for quantitative analysis of regional pulmonary perfusion. *Am J Roentgenol*. 2007;188:48–56.
73. Meier P, Zierler KL. On the theory of the indicator-dilution method for measurement of blood flow and volume. *J Appl Physiol*. 1954;6:731–744.
74. Ohno Y, Murase K, Higashino T, et al. Assessment of bolus injection protocol with appropriate concentration for quantitative assessment of pulmonary perfusion by dynamic contrast-enhanced MR imaging. *J Magn Res Imaging*. 2007; 25:55–65.
75. Risse F, Semmler W, Kauczor HU, et al. Dual-bolus approach to quantitative measurement of pulmonary perfusion by contrast-enhanced MRI. *J Magn Res Imaging*. 2006;24: 1284–1290.
76. Oldendorf WH, Kitano M, Shimizu S, et al. Hematocrit of the human cranial blood pool. *Circ Res*. 1965;17:532–539.
77. Westerhof N, Lankhaar JW, Westerhof BE. The arterial Windkessel. *Med Biol Eng Comput*. 2009;47:131–141.
78. Westerhof N, Elzinga G, Sipkema P. An artificial arterial system for pumping hearts. *J Appl Physiol*. 1971;31: 776–781.
79. Bellofiore A, Roldan-Alzate A, Besse M, et al. Impact of acute pulmonary embolization on arterial stiffening and right ventricular function in dogs. *Ann Biomed Eng*. 2012;41:195–204.
80. Stevens GR, Garcia-Alvarez A, Sahni S, et al. RV dysfunction in pulmonary hypertension is independently related to pulmonary artery stiffness. *JACC Cardiovasc Imaging*. 2012;5: 378–387.

CME-SAM EXAM INSTRUCTIONS FOR OBTAINING AMA PRA CATEGORY 1 CREDITS™

The *Journal of Thoracic Imaging* includes CME-certified content that is designed to meet the educational needs of its readers. This article is certified for 1.5 AMA PRA Category 1 Credits™. This activity is available for credit through May 31, 2014.

Accreditation Statement

Lippincott Continuing Medical Education Institute, Inc., is accredited by the Accreditation Council for Continuing Medical Education to provide continuing medical education for physicians.

Credit Designation Statement

Lippincott Continuing Medical Education Institute, Inc., designates this journal-based CME activity for a maximum of one and a half (1.5) AMA PRA Category 1 Credits™. Physicians should only claim credit commensurate with the extent of their participation in the activity.

To earn CME credit, you must read the article in *The Journal of Thoracic Imaging* and complete the quiz, answering at least 70 percent of the questions correctly. Mail the Answer Sheet to Lippincott CME Institute, Inc., Wolters Kluwer Health, Two Commerce Square, 2001 Market Street, 3rd Floor, Philadelphia, PA 19103. Only the first entry will be considered for credit, and must be postmarked by the expiration date. Answer sheets will be graded and certificates will be mailed to each participant within 6 to 8 weeks of participation.

Questions marked with an asterisk are ABR Self-Assessment Module (SAM) questions. Participants can claim credit for the SAM regardless of the test outcome. Notify the ABR of the SAM completion, or visit the ABR website at www.theabr.org to set up or log in to your personal database to record the number of SAMs you completed. The SAM ID number will be printed on the CME certificate for your records. If you wish to include the ID number in your ABR database, contact a MOC Specialist at the ABR office for instruction by calling 520-519-2152.

CME-SAM EXAMINATION

Please mark your answers on the ANSWER SHEET found on page W56 of the Web Exclusive Content in the May 2013 issue of the *Journal of Thoracic Imaging* located at www.thoracicimaging.com.

After completing this CME-SAM activity, physicians should be better able to:

- Identify the defining characteristics of pulmonary hypertension
- Identify MRI techniques best suited for evaluation of patients with known or suspected pulmonary hypertension
- Diagnose pulmonary hypertension using various imaging techniques

*1. Which of the following defines pulmonary hypertension?

- (a) Mean pulmonary artery pressure > 25 mm Hg at rest
- (b) Pulmonary capillary wedge pressure > 15 mm Hg
- (c) Pulmonary vascular resistance of < 3 Wood units
- (d) Right ventricular systolic pressure > 10 mm Hg

Please see the following reference for further study:

1. McLaughlin VV, Archer SL, Badesch DB, et al. ACCF/AHA 2009 expert consensus document on pulmonary hypertension: a report of the American College of Cardiology Foundation Task Force on Expert Consensus Documents and the American Heart Association. Developed in collaboration with the American College of Chest Physicians, American Thoracic Society, Inc., and the Pulmonary Hypertension Association. *Circulation*. 2009;119:2250–2259.

*2. What is the most common cause of acute pulmonary hypertension?

- (a) Acute myocardial infection
- (b) Acute respiratory distress syndrome
- (c) Acute pulmonary thromboembolism
- (d) Acute aortic dissection

Please see the following reference for further study:

1. Hui-li G. The management of acute pulmonary arterial hypertension. *Cardiovasc Ther*. 2011;29:153–175.

*3. Which of the following CT findings is the *most* suggestive of pulmonary veno-occlusive disease in a patient with recently diagnosed pulmonary hypertension?

- (a) Pulmonary vein enlargement
- (b) Interlobular septal thickening
- (c) Right ventricular hypertrophy
- (d) Pulmonary artery intimal calcification

Please see the following reference for further study:

1. Frazier AA, Franks TJ, Mohammed TL, Ozbudak IH, Galvin JR. From the Archives of the AFIP: pulmonary veno-occlusive disease and pulmonary capillary hemangiomatosis. *Radiographics*. 2007;27:867–882.

*4. Which of the following magnetic resonance imaging techniques is best suited for pulmonary vascular shunt quantification?

- (a) Cardiac gated steady state free precession
- (b) Contrast-enhanced magnetic resonance angiography
- (c) Time-of-flight magnetic resonance angiography
- (d) Phase contrast magnetic resonance angiography

Please see the following reference for further study:

1. Debl K, Djavidani B, Buchner S, et al. Quantification of left-to-right shunting in adult congenital heart disease: phase-contrast cine MRI compared with invasive oximetry. *Br J Radiol*. 2009;82:386–391.

*5. What best characterizes the histopathology of chronic pulmonary hypertension?

- (a) Pulmonary arterial smooth muscle hypertrophy
- (b) Pulmonary venous thrombosis
- (c) Lymphocytic infiltration of pulmonary arteries
- (d) Panlobular emphysema

Please see the following reference for further study:

1. Galie N, Hoeper MM, Humbert M, et al. Guidelines for the diagnosis and treatment of pulmonary hypertension: the Task Force for the Diagnosis and Treatment of Pulmonary Hypertension of the European Society of Cardiology (ESC) and the European Respiratory Society (ERS), endorsed by the International Society of Heart and Lung Transplantation (ISHLT). *Eur Heart J*. 2009;30:2493–2537.

*6. Which of the following chest radiographic findings is most suggestive of pulmonary hypertension?

- (a) Pulmonary hyperinflation
- (b) Splaying of the carina
- (c) Filling in of retrosternal space
- (d) Left ventricular calcification

Please see the following reference for further study:

1. Beghetti M, Galie N. Eisenmenger syndrome a clinical perspective in a new therapeutic era of pulmonary arterial hypertension. *J Am Coll Cardiol*. 2009;53:733–740.

*7. Which of the following is the reference standard imaging test for chronic pulmonary thromboembolic hypertension?

- (a) Ventilation-perfusion scintigraphy
- (b) CT pulmonary angiography
- (c) Echocardiography
- (d) MR angiography

Please see the following reference for further study:

1. Tunariu N, Gibbs SJ, Win Z, et al. Ventilation-perfusion scintigraphy is more sensitive than multidetector CTPA in detecting chronic thromboembolic pulmonary disease as a treatable cause of pulmonary hypertension. *J Nucl Med*. 2007;48:680–684.

*8. Which of the following is an independent predictor of mortality in pulmonary arterial hypertension?

- (a) Tricuspid valve regurgitant fraction
- (b) Pulmonary artery stiffness
- (c) Interventricular septal bowing
- (d) Increased right ventricular ejection fraction

Please see the following reference for further study:

1. Gan CT, Lankhaar JW, Westerhof N, et al. Noninvasively assessed pulmonary artery stiffness predicts mortality in pulmonary arterial hypertension. *Chest*. 2007;132:1906–1912.

Answer sheet can be found on page W56 of the Web Exclusive Content in the May 2013 issue of the *Journal of Thoracic Imaging* located at www.thoracicimaging.com.